AD-A104 308 DAVID W TAYLOR NAVAL SHIP RESEARCH AND DEVELOPMENT CE--ETC F/G 13/10
COMPARISON OF FULL-SCALE AND RIGID VINYL MODEL STRUCTURAL RESPO--ETC(U)
AUG 81 W H HAY
UNCLASSIFIED DTNSRDC-81/058 NL

END
DATE FILMED
10-81
DTIC

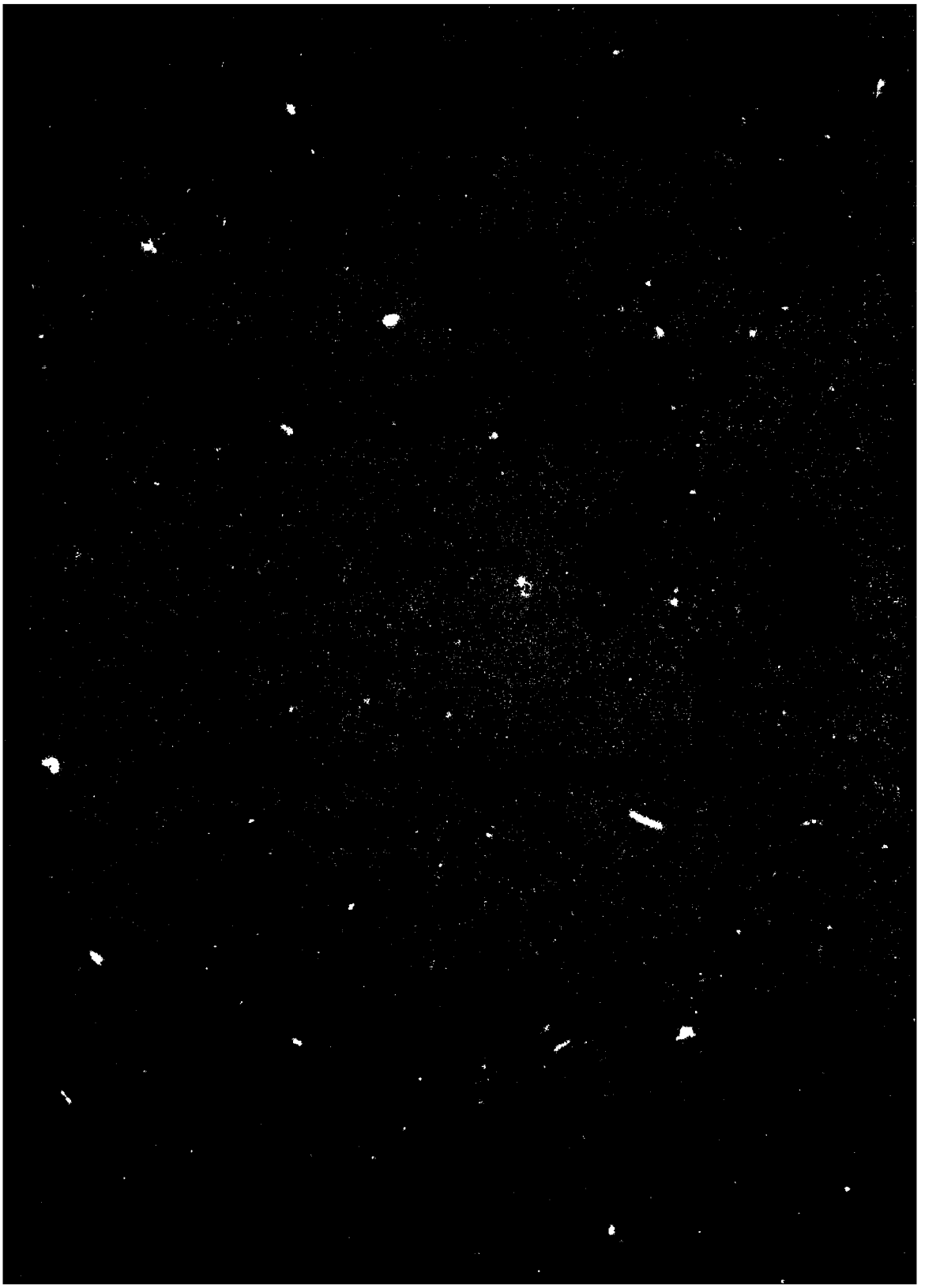

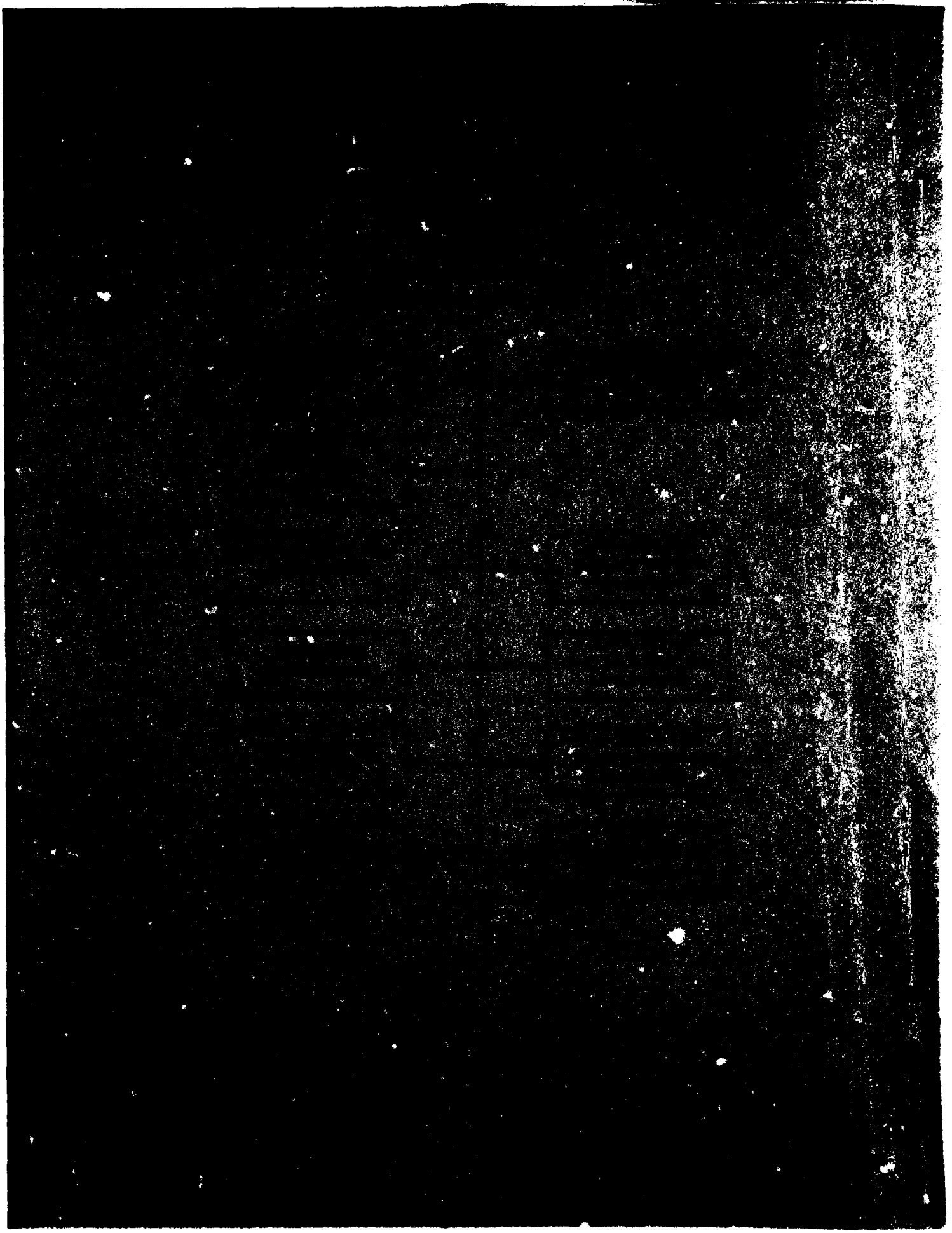

UNCLASSIFIED
SECURITY CLASSIFICATION OF THIS PAGE (When Data Entered)

REPORT DOCUMENTATION PAGE

READ INSTRUCTIONS BEFORE COMPLETING FORM

1. REPORT NUMBER	2. GOVT ACCESSION NO.	3. RECIPIENT'S CATALOG NUMBER
DTNSRDC-81/058	AD-A104308	

4. TITLE (and Subtitle)
COMPARISON OF FULL-SCALE AND RIGID VINYL MODEL STRUCTURAL RESPONSES FOR A SMALL WATERPLANE AREA TWIN HULL CRAFT (SSP KAIMALINO)

5. TYPE OF REPORT & PERIOD COVERED
Final

6. PERFORMING ORG. REPORT NUMBER

7. AUTHOR(s)
William H. Hay

8. CONTRACT OR GRANT NUMBER(s)

9. PERFORMING ORGANIZATION NAME AND ADDRESS
David W. Taylor Naval Ship Research and Development Center
Bethesda, Maryland 20084

10. PROGRAM ELEMENT, PROJECT, TASK AREA & WORK UNIT NUMBERS
(See reverse side)

11. CONTROLLING OFFICE NAME AND ADDRESS
Naval Material Command
Washington, D.C. 20360

12. REPORT DATE
August 1981

13. NUMBER OF PAGES
83

14. MONITORING AGENCY NAME & ADDRESS (if different from Controlling Office)
Naval Sea Systems Command 03R
Washington, D.C. 20362

15. SECURITY CLASS. (of this report)
UNCLASSIFIED

15a. DECLASSIFICATION DOWNGRADING SCHEDULE

16. DISTRIBUTION STATEMENT (of this Report)
APPROVED FOR PUBLIC RELEASE: DISTRIBUTION UNLIMITED

17. DISTRIBUTION STATEMENT (of the abstract entered in Block 20, if different from Report)

18. SUPPLEMENTARY NOTES

19. KEY WORDS (Continue on reverse side if necessary and identify by block number)

SWATH	Structural Loads
Small Waterplane Area Twin Hull Ship	Motions
SSP KAIMALINO	Wave Impact Pressure
Rigid Vinyl Model	

20. ABSTRACT (Continue on reverse side if necessary and identify by block number)
The need to provide the technical experience necessary to determine loads criteria for Small Waterplane Area Twin Hull (SWATH) ship design led to a structural evaluation program of the SWATH prototype craft, SSP KAIMALINO, operated by the Naval Ocean Systems Center (NOSC) and a scaled rigid vinyl/fiberglass model. The experimental prototype and model were instrumented with strain, pressure, and accelerometer transducers. Static load evaluations were conducted on both to obtain a basis for comparison
(Continued on reverse side)

DD FORM 1 JAN 73 1473 EDITION OF 1 NOV 65 IS OBSOLETE
S/N 0102-LF-014-6601

UNCLASSIFIED
SECURITY CLASSIFICATION OF THIS PAGE (When Data Entered)

(Block 10)

Task Area SF43 411 211, 19424
Work Unit 1170-098
Model Task Area SF43 422 598, 20445
Work Unit 1730-053

(Block 20 continued)

of prototype and rigid vinyl model responses and to obtain load per unit strain relationships. Prototype and model static strain data indicate that for the lower hulls and vertical struts agreement is good; for the upper hull, however, agreement is inconsistent and, at best fair. It is believed that simplifications made in scaling the model structure were responsible for these inconsistencies. Load/strain sensitivities developed from the static load evaluations are applied to strain data collected during sea trials to establish a trials derived loads data base. Estimates are then made of wave induced primary side loads for various sea states and headings. For a 20 year operational lifetime the maximum side loads are predicted to be approximately one-half the craft displacement. Agreement of the model and prototype based loads data is excellent and further validates rigid vinyl modeling as a design tool for estimating full-scale loads.

Accession For
NTIS GRA&I [X]
DTIC T4B [ ]
Unannounced [ ]
Justification
By
Distribution/
Availability Codes
Dist | Avail and/or Special
A

TABLE OF CONTENTS

LIST OF FIGURES

LIST OF TABLES

NOTATION

A	Enclosed overall area, ft^2
A_s	Section area, $in.^2$
a	Acceleration, ft/sec^2
b	Location of strain bridge in stabilizer end connection, in.
$\mathcal{L}$	Longitudinal centerline
c	Fluid density scale factor
C_o	Stabilizer neutral axis location along craft centerline, in.
C_1	Stabilizer neutral axis location near end connection, in.
d	Location of vertical static load applied to stabilizer, in.
E	Modulus of elasticity, $lb/in.^2$ (psi)
EI	Bending rigidity, lb $in.^2$
e	Ratio of moduli of elasticity
F	Applied force, lb
f	Frequency, Hz
G	Shear modulus, $lb/in.^2$ (psi)
H	Prototype to model thickness scale ratio
$H_{1/3}$	Average of the one-third highest variation--significant value
$H_{1/10}$	Average of the one-tenth highest variation
h	Local plating thickness, in.
I_A	Area moment of inertia, $in.^4$
I_m	Mass moment of inertia, lb $in.^2$
K, k	Spring constants, lb/in.

L l	Length, ft or in.
M M_B	Bending moment, in. lb
M_e	End moment, in. lb
M_o	Vertical bending moment based on strains measured at stabilizer centerline, in. lb
M_l	Vertical bending moment based on strains measured in stabilizer end connection, in. lb
m	Mass, lb sec^2/in. or lb sec^2/ft
m	As a subscript refers to model
P	Vertical load, lb
P_C	Vertical load acting on canard, lb
P_r	Pressure, lb/$in.^2$ (psi)
p	As a subscript refers to prototype
R	Degree of end fixity
S	Section modulus, in.
T	Torque, lb
t	Time, sec
V	Velocity, ft/sec
W	Vertical load, lb
W_s	Vertical load on stabilizer, lb
γ	Non-dimensional constant related to spring constant
δ	Deflection, in.
ε	Strain, μin./in.
ε_{SHAFT}	Strain measured in canard shaft, μin./in.
ε_o	Strain measured at stabilizer centerline, μin./in.

ε_1	Strain measured in stabilizer end connection, μin./in.
θ	Angle, rotation, deg
λ	Overall prototype to model scale factor
ρ	Fluid density, lb $sec^2/in.^4$ or lb sec^2/ft^4
σ	Stress, $lb/in.^2$ (psi)
ω	Circular frequency, rad/sec

LIST OF ABBREVIATIONS

DTNSRDC	David W. Taylor Naval Ship Research and Development Center
MASK	Maneuvering and Seakeeping Facility
NOSC	Naval Ocean Systems Center
RAO	Response Amplitude Operator
SSP	Stable Semi-Submerged Platform
SWATH	Small Waterplane Area Twin Hull
T&E	Test and Evaluation

ABSTRACT

The need to provide the technical experience necessary to determine loads criteria for Small Waterplane Area Twin Hull (SWATH) ship design led to a structural evaluation program of the SWATH prototype craft, SSP KAIMALINO, operated by the Naval Ocean Systems Center (NOSC) and a scaled rigid vinyl/fiberglass model. The experimental prototype and model were instrumented with strain, pressure, and accelerometer transducers. Static load evaluations were conducted on both to obtain a basis for comparison of prototype and rigid vinyl model responses and to obtain load per unit strain relationships. Prototype and model static strain data indicate that for the lower hulls and vertical struts agreement is good; for the upper hull, however, agreement is inconsistent and at best fair. It is believed that simplifications made in scaling the model structure were responsible for these inconsistencies. Load/strain sensitivities developed from the static load evaluations are applied to strain data collected during sea trials to establish a trials derived loads data base. Estimates are then made of wave induced primary side loads for various sea states and headings. For a 20 year operational lifetime the maximum side loads are predicted to be approximately one-half the craft displacement. Agreement of the model and prototype based loads data is excellent and further validates rigid vinyl modeling as a design tool for estimating full-scale loads.

ADMINISTRATIVE INFORMATION

Work performed in support of prototype testing was funded by the Ship Concepts Development Group (Code 31R) of the Naval Sea Systems Command under Task Area SF43 411 211, Task 19424. The work was carried out by the David W. Taylor Naval Ship Research and Development Center (DTNSRDC) under Work Unit 1170-098. Model testing was funded by the Hull Research Technology Office (Code 32R) of the Naval Sea Systems Command as part of the Surface Ships Structures block, Task Area SF43 422 598, Task 20445. This work was conducted at DTNSRDC under Work Unit 1730-053.

METRIC EQUIVALENCE

United States customary units are used throughout this report. The following conversion factors can be used to obtain the equivalent value in the International System (SI) units.

	U.S. Units	Equivalent SI Units
Length	inch (in.) foot (ft)	2.54 centimeters (cm) 0.3048 meter (m)
Mass	pound (lb)	0.45359 kilogram (kg)
Stress	pounds per square inch (psi)	6894.8 Pascals (Pa)
Force	pound (lb)	4.448 Newtons (N)
Strain	microinches per inch (μin./in.) a nondimensional term	1000 nano meters per meter (nm/m)
Speed	knots	1.852 kilometers/hour (km/hr)
Pressure	pounds per square in. (psi)	6894.8 Pascals (Pa)

INTRODUCTION

As part of a continuing program to develop multi-hull ship technology, the David W. Taylor Naval Ship Research and Development Center (DTNSRDC) is currently investigating the structural, hydrodynamic, vibrational, and seakeeping capabilities of the Small Waterplane Area Twin Hull (SWATH) ship concept. The investigations have taken the form of full-scale SWATH prototype trials with the 190 ton stable semi-submerged platform (SSP KAIMALINO) and extensive scale model studies. The general configuration and characteristics of the KAIMALINO prototype are shown in Figure 1.

The primary objective of the structural portion of the test and evaluation (T&E) program was the development of a sea loads data base from which loads criteria for future SWATH ship designs could be validated. To develop this loads data base, load per unit of structural strain relationships derived from static load evaluations were applied to structural response data collected during seakeeping trials. Irregular wave sea trials were conducted on both the prototype craft and a one-tenth scale rigid vinyl/fiberglass structural model. Data collected were also used to assess the capability of rigid vinyl modeling in predicting full-scale structural responses and loads.

Results of the structural T&E are summarized as are comparisons of structural behavior between the KAIMALINO prototype and model. In addition, predictions are made of sea induced loads for conditions other than those of the seakeeping trials.

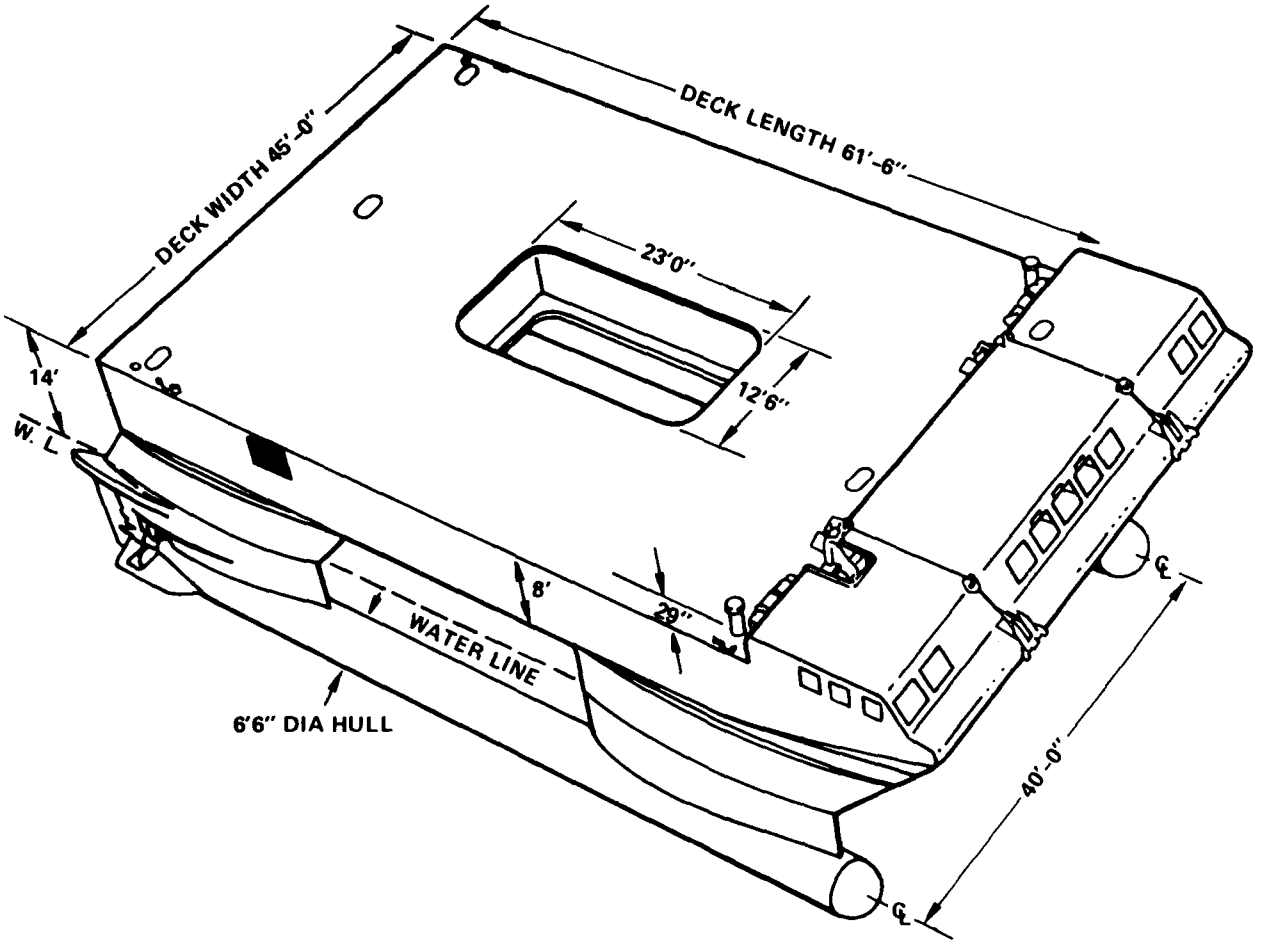

OVERALL LENGTH	88'-4"
OVERALL WIDTH	48'-8"
OVERALL HEIGHT	31'-9"
DRAFT	15'-3"
DISPLACEMENT	190 TONS
MAX SPEED	25 KNOTS
RANGE	450 NAUT. MIL

Figure 1 - SSP KAIMALINO General Arrangement

PROTOTYPE DESIGN AND CONSTRUCTION

The SSP KAIMALINO is the Navy's prototype test vehicle of the SWATH ship concept. It was built by the U.S. Coast Guard at the Curtis Bay shipyard for the Naval Oceans Systems Center (NOSC). Ship construction was started in December 1971 and completed in 1973.

The SSP has two torpedo shaped lower hulls which are totally submerged (Figure 1). The upper hull cross structure is connected to these lower hulls by four vertical surface piercing struts designed to minimize craft waterplane area. Lower hulls and vertical struts are constructed of 50,000 psi steel; the cross structure is built of 5086 aluminum. The cross structure to vertical strut connection is by means of an explosively bonded Deta Clad joint. The KAIMALINO is equipped with submerged bow and stern horizontal control surfaces. Located inboard on the bows of the lower hulls are fully controllable canards. In the stern a full span stabilizer was constructed between the lower hulls with controllable flaps along the trailing edge. Use of these control surfaces combined with the small waterplane area provides for unique control of craft motions.[1*]

MODEL DESIGN AND CONSTRUCTION

A one-tenth scale composite rigid vinyl and fiberglass model of the KAIMALINO was designed and built by Atkins and Merrill, Inc., for DTNSRDC evaluation. Fiberglass-foam sandwich material was used for simulating prototype steel in the lower hulls, vertical struts, and aft stabilizer. Rigid vinyl was used for simulating aluminum in the upper hull. Table 1 summarizes material properties of the prototype and model.

The scaling analysis employed for the overall design and construction of the model was based on dynamic Froude scaling laws. Prototype to model lengths, λ, were scaled as 10.0; fluid density ratio, c, was considered equal to 1.0; and accelerations were scaled one to one. Based on these fundamental scaling relationships, secondary scale factors such as mass, force, and velocity were derived; Table 2 gives a complete list of the fundamental and derived Froude scaling factors applicable to the model.

For structural responses, it was desired that model strains equal prototype strains; thus, a second set of fundamental scaling relationships was introduced for

*A complete listing of references is given on page 71.

TABLE 1 - MATERIAL PROPERTIES OF KAIMALINO PROTOTYPE AND MODEL

	Upper Hull			Lower Hull, Vertical Struts		
	Material	Modulus of Elasticity E, psi	Shear Modulus G, psi	Material	Modulus of Elasticity E, psi	Shear Modulus G, psi
Prototype	Aluminum	10.0×10^6	4.0×10^6	Steel	30.0×10^6	12.0×10^6
Model	Rigid Vinyl	0.45×10^6	0.18×10^6	Fiberglass	3.0×10^6	1.2×10^6

scaling structural quantities. Where strains scale one to one, the ratio of prototype to model elastic moduli is e, and the ratio of prototype to model local plating thicknesses h_p/h_m is designated as H. To ensure scaled dynamic responses, the following provision is placed on the thickness scale ratio H:

$$\sigma = \frac{F}{A} = \frac{F}{Lh} \tag{1}$$

where σ = material stress

F = externally applied force

A = structural area

L = length

h = thickness

The ratio of prototype to model stress is as follows (subscript p refers to the KAIMALINO prototype and subscript m to the model):

$$\frac{\sigma_p}{\sigma_m} = \frac{E_p \varepsilon_p}{E_m \varepsilon_m} = (e)(1.0) = \frac{\frac{F_p}{f_m}}{\left(\frac{L_p}{L_m}\right)\left(\frac{h_p}{h_m}\right)} = \frac{c\lambda^3}{\lambda H}$$

where E = modulus of elasticity

ε = material strain

c = fluid density ratio

TABLE 2 - FROUDE SCALING SIMILITUDE LAWS

Measurand	Notation	Scale Factor
Length	L_p/L_m	λ*
Fluid Density	ρ_p/ρ_m	c**
Acceleration	a_p/a_m	1.0
Mass	m_p/m_m	$c\lambda^3$
Time	t_p/t_m	$\sqrt{\lambda}$
Mass Moment of Inertia	I_{mp}/I_{mm}	$c\lambda^5$
Force	F_p/F_m	$c\lambda^3$
Bending Moment	M_p/M_m	$c\lambda^4$
Torque	T_p/T_m	$c\lambda^4$
Velocity	V_p/V_m	$\sqrt{\lambda}$
Enclosed Area	A_{EP}/A_{Em}	λ^2
Pressure	P_p/P_m	$c\lambda$
Deflection	δ_p/δ_m	λ
Angle	θ_p/θ_m	1.0

*For this model, λ = 10.0.

**For these tests, c is assumed to be 1.0.

Thus

$$H = \frac{c\lambda^2}{e} \tag{2}$$

From the fundamental structural scaling relationships, scale factors for structural areas, area moments of inertia, bending rigidity and section moduli are derived (Table 3).

TABLE 3 - STRUCTURAL SCALING LAWS

Measurand	Notation	Scale Factor
Strain	$\varepsilon_p/\varepsilon_m$	1.0
Modulus of Elasticity	E_p/E_m	e*
Plating Thickness	h_p/h_m	$H = c\lambda^2/e$
Stress (Bending and Shear)	σ_p/σ_m	e
Section Area	A_{sp}/A_{sm}	$c\lambda^3/e$
Area Moment of Inertia	I_{Ap}/I_{Am}	$c\lambda^5/e$
Bending Rigidity**	E_pI_p/E_mI_m	$c\lambda^5$
Section Modulus**	S_p/S_m	$c\lambda^4/e$

*e = 10 for lower hulls, vertical struts, and control surfaces e = 22.2 for upper hull.

**For overall responses only--does not apply to plating alone.

Model weight and location of the center of gravity were scaled from the prototype operational displacement (190 tons), and draft (15 feet 3 inches) by placing lead shot ballast in the model lower hulls and lead weights on the weather deck. An electric motor was fitted in each lower hull, thus providing the model with propulsion during seakeeping trials. Servo mechanisms added the capability of control of the model canards, stabilizer flaps, and rudders.

TEST INSTRUMENTATION

To acquire overall structural response data for the SSP KAIMALINO prototype, 24 strain gage bridges were located on principal structural members. Measurements of stress concentrations, while important, were avoided because they are not indicative of primary structural loads. The strain gages were Micro-Measurement type EA-06-125AD-120 for steel and EA-13-125AD-120 for aluminum. The original gages were installed during construction of the vessel at the Curtis Bay Coast Guard Yard; additional gages were installed just prior to the sea trials. Strain bridge locations are shown in Figure 2, and listed in Table 4.

Strain gage bridge locations for the model were scaled from those of the prototype with the following differences:

1. an overall upper hull transverse bending bridge was installed on the model at Frame 19 (S25), and

2. the canard shaft bending bridge (S7) was excluded.

Strain gages used for the model were BLH type FAE-18-12S3 for fiberglass and FAE-18-12S36 for rigid vinyl.

Additional instrumentation was installed in the model, including pressure gages, roll and pitch gyros, and accelerometers. As shown in Figure 2, six pressure gages were installed on the model to monitor wave impact pressures on the upper hull; four were installed in the "V" bow bottom forward of Bulkhead 13, and two were installed in the flat cross structure bottom aft of Bulkhead 13. Accelerometers were mounted to record bow, center of gravity, and port midship vertical accelerations (Figure 2).

STATIC STRUCTURAL EVALUATIONS

VERTICAL STRUT SIDE LOAD

Procedure

To provide the design community with the trials-based sea loads information necessary for developing reliable loads criteria, it was first necessary to accurately define the structural response to a known load. The ratio of load to response could then be used in conjunction with structural responses derived during sea trials to estimate sea-induced loads. The most reliable means for defining structural response to a known load is through a static structural evaluation of the test craft, that is by applying a known static load, and recording strain

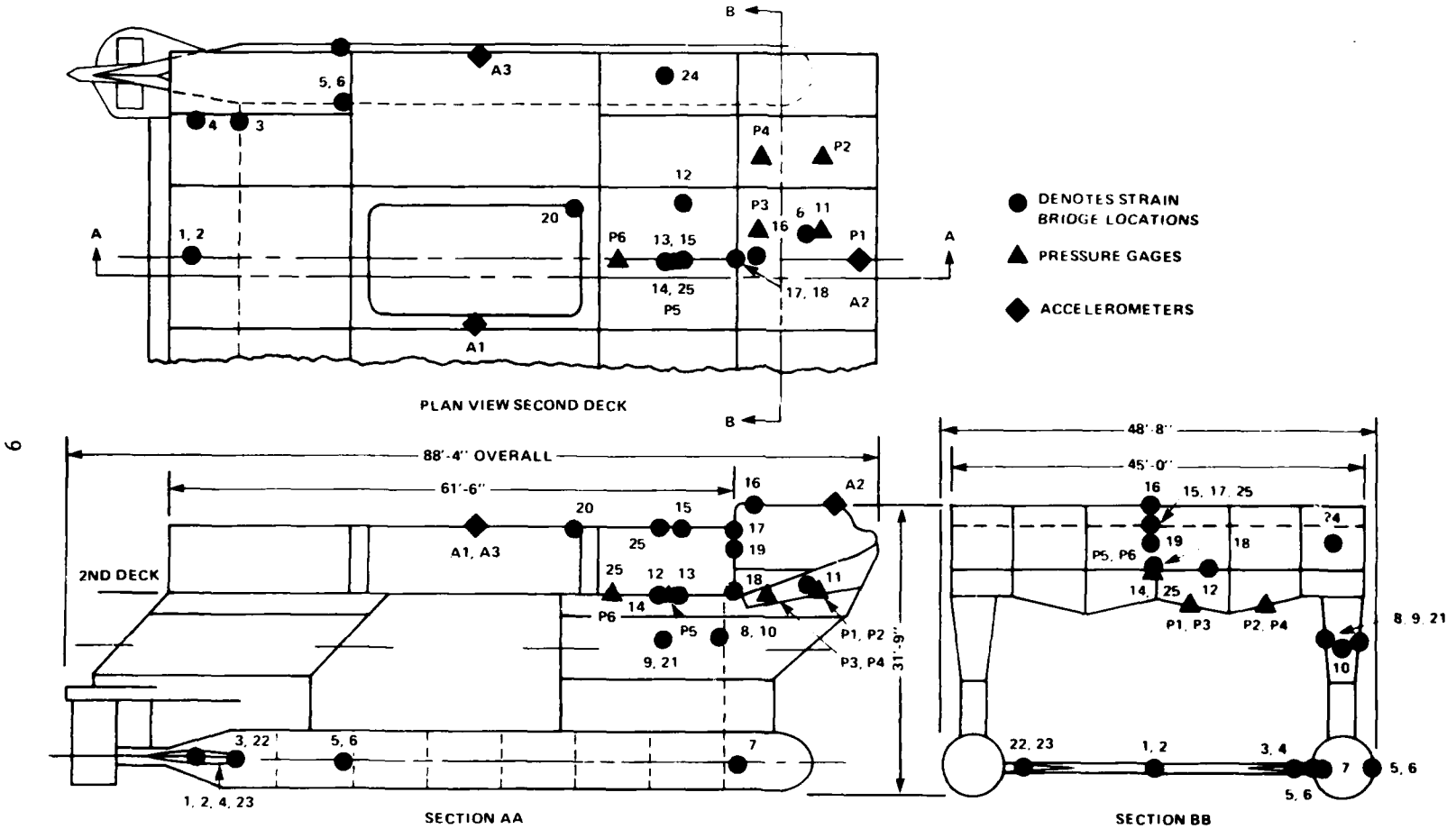

Figure 2 - SSP KAIMALINO Prototype and Model Transducer Locations

TABLE 4 - TRANSDUCER LOCATIONS FOR SSP KAIMALINO PROTOTYPE AND MODEL

Gage Number	Measurement	Test Monitored			
		Prototype		Model	
		Static Evaluation	Dynamic Trials	Static Evaluation	Dynamic Trials
1	Stabilizer vertical bending, midspan	X			
2	Stabilizer axial strain, midspan			X	X
3	Stabilizer lateral bending, port end	X		X	X
4	Stabilizer vertical bending, port end	X		X	X
5	Lower hull lateral bending, BHD V	X		X	X
6	Lower hull torsion, BHD V	X		X	X
7	Canard shaft vertical bending	X	X		
8*	Forward strut lateral bending, BHD E	X	X	X	X
9*	Forward strut lateral bending, mid-chord	X	X	X	X
10	Forward strut shear, BHD E			X	X
11	Plating strain, pressure, Fr. 6½				X
12	Second deck vertical bending, Fr. 17 near long. BHD	X		X	X
13*	Second deck vertical bending, Fr. 17 on ℄	X	X	X	X
14	Plating strain, pressure, Fr. 17½		X		X
15*	Main deck vertical bending, Fr. 17 on ℄	X	X	X	X
16	0½ level vertical bending, BHD 13			X	X
17*	Main deck vertical bending, BHD 13	X	X	X	X
18*	Second deck vertical bending, BHD 13	X	X	X	X
19	Vertical shear, BHD 13			X	X
20	Stress concentration, well coaming				X
21	Forward strut torsion	X			
22	Stabilizer lateral bending, starboard end			X	X
23	Stabilizer vertical bending, starboard end			X	X
24*	Forward strut column support axial strain	X	X	X	X
25	Upper hull transverse bending, Fr. 19			X	X

*Denotes primary strain bridges.

bridge outputs. Since the same methodology is used in full-scale and model testing, the load per unit strain sensitivities that are derived can also be of considerable value in providing a data base for evaluating how well the model simulates the complex structural behavior of the full-scale craft.

For the side load static evaluation of the KAIMALINO prototype a known static load was applied incrementally between the forward struts while strain bridge outputs were recorded. To simulate sea induced loads the static load was applied, using a large diameter steel pipe with an in line hydraulic jack and load cell, to the center of lateral pressure for each strut (Figure 3). Local structural buckling was prevented by applying the load on a continuous transverse bulkhead (Bulkhead E), using an exterior load spreading pad, and stiffening the local structure. To prevent the development of reaction forces in the keel blocks, the evaluation was conducted with the KAIMALINO floating freely.

The magnitude of the static load was based on a NOSC design estimate for maximum forward strut lateral shear. A simple frame analysis performed by DTNSRDC indicated that a 60 kip per strut load would produce measurable, yet safe, structural responses in all pertinent bridges. During the initial loading critical welds were closely observed, and selected strain bridges, as well as the deflection between struts, were monitored for nonlinearity or dangerously high values.

A scaled forward strut evaluation was also conducted on the model. With the model floating freely, a scaled load of 60 pounds was applied laterally between the forward struts. Due to the proportionally higher strength of the model local structure, only a small load spreading pad was necessary to prevent local damage.

To develop the load per unit strain sensitivity of each bridge to a total side load (i.e., a side load distributed equally between forward and aft struts), it was necessary to define the structural response of each bridge to separate forward and aft strut static loadings. In lieu of performing a second set of expensive, time consuming static tests on the prototype, the aft static loading was conducted only on the model. As was the case for the forward strut, the load was scaled to 60 pounds and applied laterally between the aft struts at the approximate center of lateral pressure while recording strain bridge responses (Figure 3).

Results

To establish the linearity and repeatability of the prototype strain bridge data, five equal static loads were applied incrementally to the forward struts.

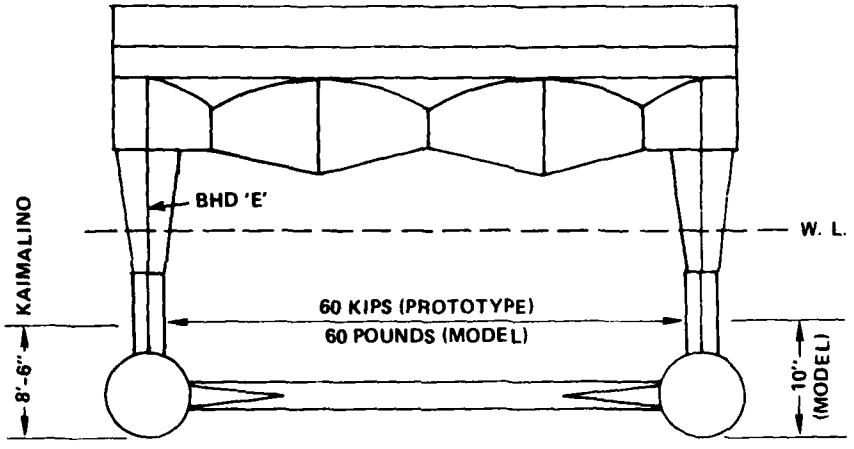

Figure 3a - Forward Strut Static Evaluation (Prototype and Model)

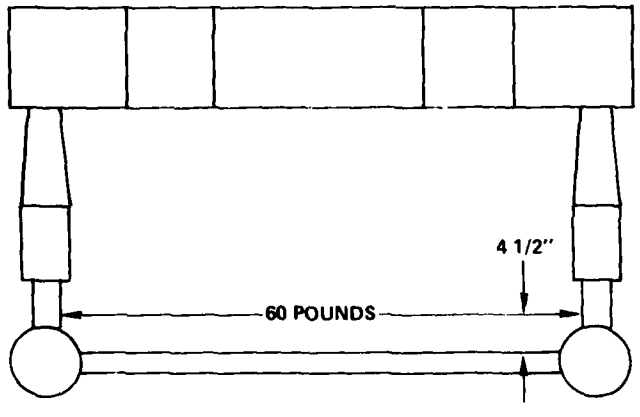

Figure 3b - Aft Strut Static Evaluation (Model)

Figure 3 - Vertical Strut Static Evaluation of KAIMALINO Prototype and Model

To avoid distortion of the strain data by locked-in construction stresses, readings from the initial loadings sequence were disregarded. Analysis of strain data from the remaining loadings proved to be both linear and repeatable throughout the load range; Table 5 summarizes the averaged strains for the 60,000 pound full- scale load. For an aft strut loading case, full-scale strain values have been calculated from model data and are also summarized in Table 5. The application of this data for obtaining prototype and model loads data is discussed later.

Strain data for the model were acquired in a similar manner. Distortion of the data due to locked-in stresses was avoided by conducting the evaluation at the conclusion of the seakeeping trials. Resulting model strain values were both linear and repeatable; Table 5 summarizes averaged strains for the 60 pound load.

A comparison of prototype and model structural responses reveals agreement in lower hull and vertical strut strains, however, there are inconsistencies in upper hull strains. There is an indication of different load paths between the prototype and model for loads being transferred from the struts to the upper hull. It is believed that the inconsistencies are the result of the use of solid sheet bulkheads in the model "V" bow, rather than trusswork as in the prototype. The solid bulkheads permitted a higher proportion of the load to be transferred into the model bow area; consequently, less load was transferred to the upper hull box structure aft of Bulkhead 13. In addition, the shear lag may have been different in the model than in the prototype due to distorted model plating thicknesses, or because of actual out-of-flatness in the prototype plating. Despite the inconsistencies, the model proved to be an excellent stress sensor for the lower hulls and vertical struts; moreover, the poor strain agreement of the upper hull has no effect on the value of the model as a load sensor.

Analysis of model strains from the aft strut loading also proved to be linear and repeatable for several load sequences. Table 5 summarizes the averaged strains for the 60 pound loading.

Load Per Unit Strain Sensitivity

To simulate sea loads acting simultaneously on all struts, the model forward and aft strut static loads were mathematically superimposed to create a single total side load acting equally on all struts. Strains for this combined total side load are the algebraic sum of the individual strain bridge responses to forward

TABLE 5 - VERTICAL STRUT STATIC EVALUATION STRUCTURAL RESPONSES OF KAIMALINO PROTOTYPE AND MODEL

Bridge No.	Location	Forward Strut Evaluation*		Aft Strut Evaluation*		Total Strains**		Load/Strain Sensitivity	
		Prototype (μin./in.)	Model (μin./in.)	Prototype (μin./in.)	Model (μin./in.)	Prototype (μin./in.)	Model (μin./in.)	Prototype (kips/μin./in.)	Prototype (kips/μin./in.)
2	Stabilizer axial	—	+3.5	—	+8.0	—	+11.5	—	10.47
5	Lower hull lateral bend.	-23.4	-18.8	+4.6	+3.7	-18.8	-15.5	6.38	7.99
6	Lower hull torsion	+15.7	+18.0	+4.8	+5.5	+20.5	+23.5	5.85	5.10
8	Fwd. strut lateral bend.	-51.5	-54.8	+5.0	+5.3	-46.5	-49.5	2.60	2.42
9	Fwd. strut lateral bend.	-35.8	-39.5	+4.1	+4.5	-31.7	-35.0	3.79	3.42
12	Second DK bend. Fr. 17	+42.6	+69.8	-3.5	-5.7	+39.1	+64.1	3.07	1.87
13	Second DK bend. ℄ Fr. 17	+32.7	+77.0	0	0	+32.7	+77.0	3.67	1.55
15	Main DK bend. ℄ Fr. 17	-23.9	-46.7	0	0	-23.9	-46.7	5.02	2.55
16	0½ Level bend. ℄ Bhd 13	—	-23.4	—	0	—	-23.4	—	5.13
17	Main DK bend. ℄ Bhd 13	-26.0	-40.5	0	+0.5	-26.0	-40.0	4.62	3.01
18	Second DK bend. ℄ Bhd 13	+120.8	+87.9	0	0	+120.8	+87.9	0.99	1.37
24	Diagonal column axial	+157.2	+135.9	-13.0	-11.2	+144.2	+124.7	0.84	0.96
25	Upper hull bend. Fr. 19	—	+51.9	—	0	—	+51.9	—	2.31

*Responses for loads of 60 kips and 60 lbs (model).
**Due to superposition of fwd and aft strut loadings.

and aft strut static loads. The model load per unit strain sensitivities were then determined by taking the ratio of the total load (120 pounds for the model) to the derived total strain. These ratios are presented in Table 5.

To develop similar total side load sensitivities for the prototype an aft strut loading data base had to be generated. The assumption was made that prototype aft strut load responses were proportional to model aft strut load strains in the same ratio as the prototype and model forward strut load strains. It is important to note that the strain outputs due to the loading of the aft strut are generally small relative to the strains obtained from the forward strut loading. Thus the error that occurs in the prototype data from using the corrected model strains is expected to be insignificant. Prototype structural responses predicted in this manner are included in Table 5. Using the forward and aft strut loading data, strain bridge sensitivities to the total side load were calculated in terms of load per unit strain (Table 5).

CONTROL SURFACE VERTICAL LOADS

Canard Shaft

To develop a data base from which control surface loads critieria could be determined, static load calibrations of prototype and model control surfaces were also performed. For the canard evaluation, a concentrated vertical load of 3000 pounds was applied incrementally near the canard tip, using a hydraulic jack and load cell (Figure 4), while outputs from the canard shaft bending bridge (Bridge S7) were recorded. The magnitude of this load was derived from studies by Stahl and Pritchett.[2]

The applied moment and measured strain data from the static canard loading was used to develop a total load per unit strain relationship.

The following are the major results of the canard evaluation:

$$M_B = 2900\varepsilon_{SHAFT} \tag{3}$$

where ε_{SHAFT} is the measured bending strain in the canard shaft in microinches per inch and M_B is the moment on the canard shaft at the inboard bearing in inch-pounds,

and

$$P_C = 85.2\varepsilon_{SHAFT} \tag{4}$$

where P_C is the total load on the canard, in pounds, due to hydrodynamic lift and slamming, assuming a net force acting at the centroid of area for the canard (34 inches from the inboard bearing).

A calibration of the model canard was not possible due to the inaccessibility of a canard shaft that could be instrumented.

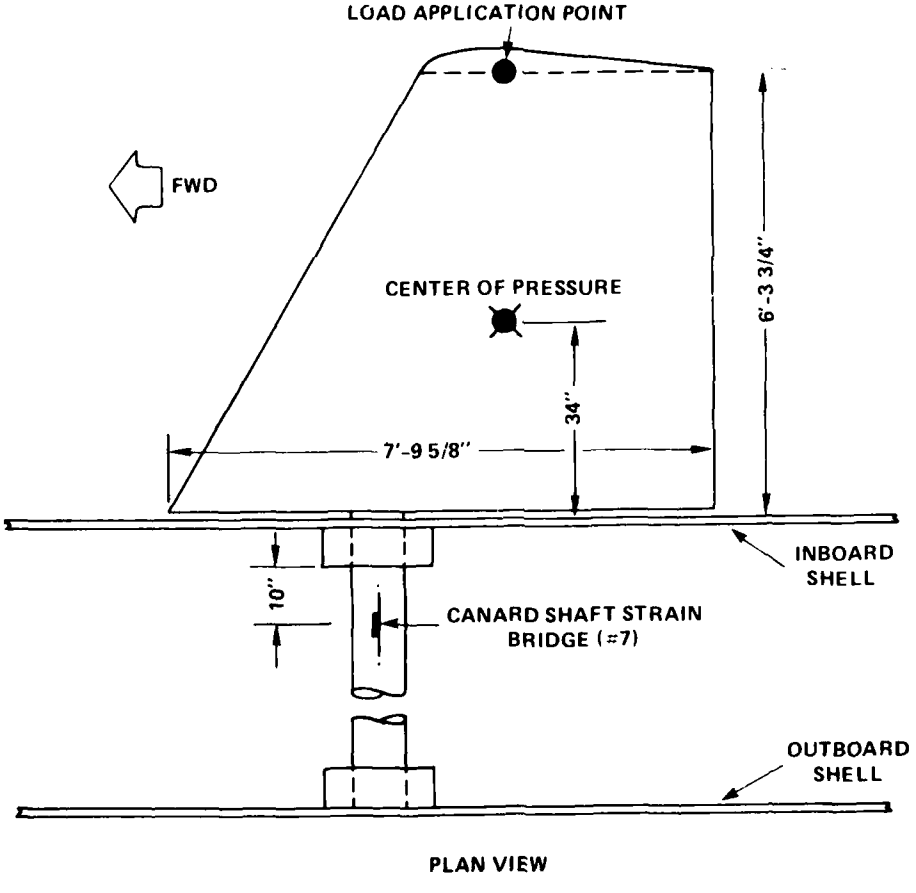

Figure 4 - Canard Static Evaluation of KAIMALINO Prototype

Aft Stabilizer

To develop the load-strain relationship for the prototype aft stabilizer, vertical static loads of 20,000 pounds were applied to the stabilizer using a pair of hydraulic jacks. The jacks were placed either side of the stabilizer centerline at the intersection of longitudinal and transverse bulkheads (Figure 5).

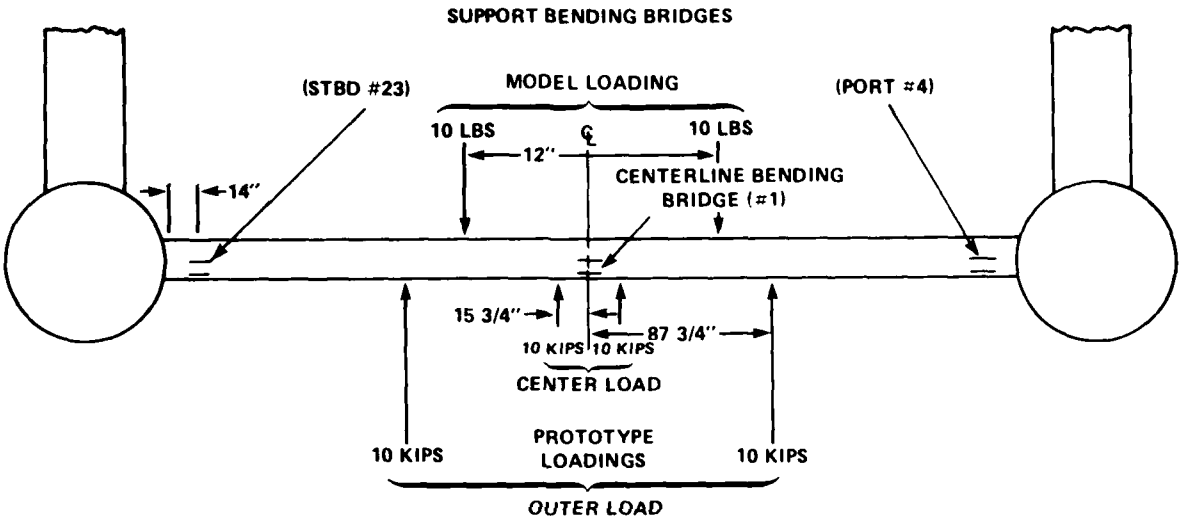

Figure 5 - Aft Stabilizer Static Evaluations of KAIMALINO Prototype and Model

Two loadings were conducted on the stabilizer by placing the jacks 15 3/4 inches and 87 3/4 inches on either side of the craft centerline. Stabilizer vertical bending and axial strains were recorded, results are shown in Figure 6.

In order to calculate the expected natural frequency of the stabilizer, the end fixity of the stabilizer-lower hull intersection had to be determine. Based on the concentrated static load strain response data, end fixity may be calculated (Appendix A). Using the derived end restraints, stabilizer natural frequency in water was also determined (Appendix B).

The major results of the prototype stabilizer evaluation are:

1. The stabilizer end moment is 67 percent of the moment for a fixed beam for any loading that is symmetric about the centerline.

Figure 6 - Aft Stabilizer Strain Bridge Sensitivity to Vertical Static Loadings

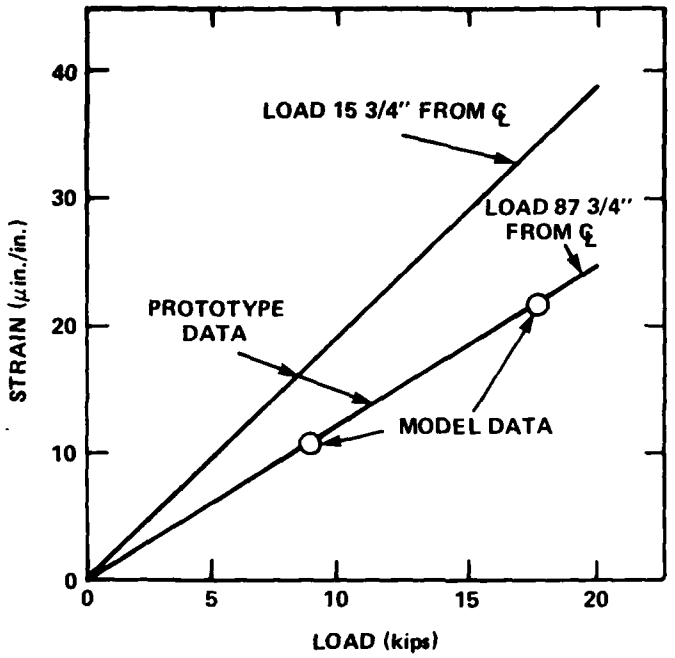

Figure 6a - Vertical Bending--Port End Connection

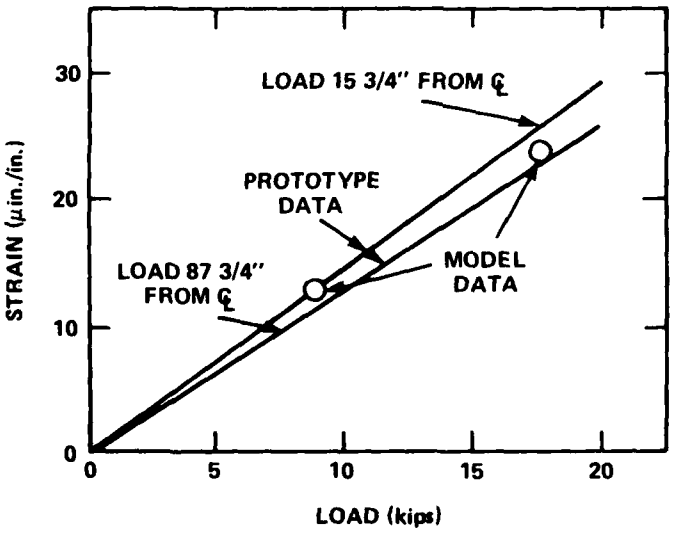

Figure 6b - Vertical Bending--Starboard End Connection

Figure 6 (Continued)

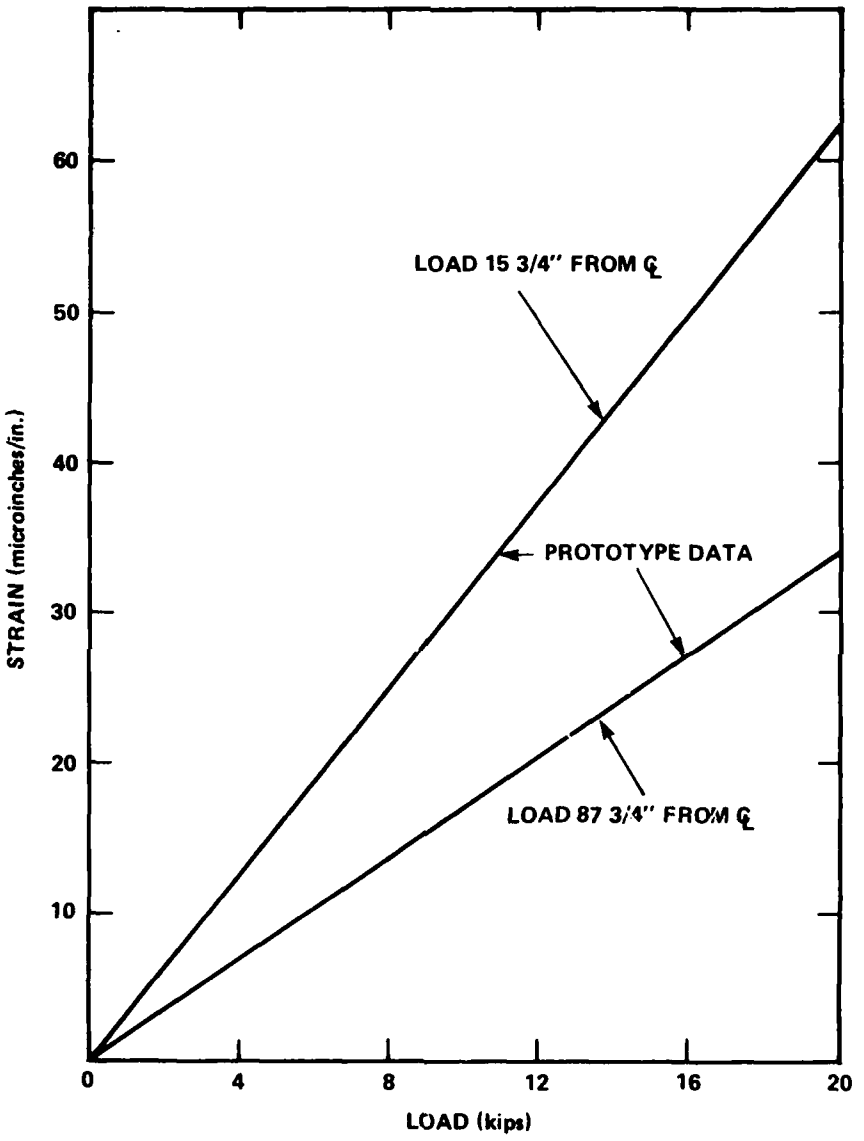

Figure 6c - Vertical Bending--Centerline

2. Relationships to convert strains measured at the stabilizer centerline or near either end connection to uniform load on the stabilizer are:

$$W_s = 652.0\times10^6\varepsilon_o$$

and

$$W_s = 1047.0\times10^6\varepsilon_1 \qquad (5)$$

where W = total load of a uniform load on the stabilizer, in pounds,

ε_o = measured strain at the centerline, in microinches per inch, and

ε_1 = measured strain near either end connection, in microinches per inch.

3. The natural frequency of the stabilizer in water is estimated at 6.8 Hz.

A scaled stabilizer static loading was also performed on the model. With the model floating freely, 10 pound brass weights were placed on the stabilizer, transversely about the stabilizer centerline, and strain bridge responses recorded. Measured model strains are plotted in Figure 6. Unfortunately, the model centerline stabilizer strain bridge malfunctioned prior to these tests precluding comparison with corresponding prototype strains. Agreement between the model and prototype end connection strains, however, is considered to be excellent. Based on the end connection strains, stabilizer end fixity of the model was calculated at 59 percent fixed (Appendix A). This value agrees well with the prototype stabilizer end fixity. Using this model end fixity, the relationship between total uniform prototype load and model end connection strain is as follows:

$$W_{PROTOTYPE} = (1100\times10^6)\varepsilon_{MODEL} \qquad (6)$$

This relationship is well within ten percent of the prototype result, and from the perspective of an experimental measurement, is considered excellent.

SEAKEEPING TRIALS

MODEL TESTS

Primary Responses

A comprehensive model test program was conducted during June 1974 in the DTNSRDC Maneuvering and Seakeeping (MASK) facilities. Trial runs were performed at

various headings in irregular waves at scaled prototype speeds of 4 and 18 knots in simulated Sea States 4 and 5. Table 6 summarizes model test conditions and Table 7 provides a definition of sea state conditions. During the testing the self propelled model was remotely controlled from the model basin test carriage and, with the exception of an umbilical cord of transduce cables, unrestrained. Control surfaces were adjusted prior to each run and fixed during the course of the run. Wave height was measured by a sonic probe fixed on the forward portion of the test carriage.

TABLE 6 - TEST CONDITIONS FOR MODEL TRIALS

Run Numbers	Heading	Scaled Speed (knots)	Scaled Sea State
1 - 3	Head	4	4
4 - 15	↓	18	4
16 - 18	↓	4	5
19 - 30	↓	18	5
31 - 33	Bow	4	4
34 - 45	↓	18	4
46 - 48	↓	4	5
49 - 60	↓	18	5
76 - 78	Stern Quarter	4	5
79 - 90	↓	18	5
106 - 108	Beam	4	5
109 - 120	↓	18	5
136 - 138	Following	4	5
139 - 144	↓	18	5
145 - 161	Head	18	5
162	↓	1	5

From a simple peak analysis of runs for each test condition, it was found that low speed, beam sea headings produced the maximum primary structural response per foot of wave height. Detailed analysis was therefore confined to these runs.

Spectral analysis provides a useful method for deriving general response characteristics of a full-scale ship or model to a random wave environment. Andrews and Dinsenbacher[3,4] give detailed accounts of the methodology of spectral analysis. Typical spectral plots for selected model strain bridges (i.e., S8 and S24) and wave height are shown in Figure 7 for low speed beam seas. All model data are presented in full-scale units to facilitate comparison with prototype data.

TABLE 7 - DEFINITION OF SEA CONDITIONS

Description	Beaufort	Range (knots)	Wind Velocity (knots)	Sea State	Wave Height (ft) Average	Wave Height (ft) Significant	Wave Height (ft) Average 1/10 Highest	Significant Range of Periods (sec)	T_{max} (Period of Maximum Energy of Spectrum)	$\bar{T}$ (Average 'Period')	$\bar{L}$ (Average 'Wave Length')	Minimum Fetch (nautical miles)	Minimum Duration (hrs)
Calm	0	0-1	0[a]	0	0	0	0	--	--	--	--	--	--
Light Air	1	1-3	2	0	0.05	0.08	0.10	Up to 12 sec	0.7	0.5	10 in.	5	10 min
Light Breeze	2	4-6	5	1	0.12	0.29	0.37	0.4-2.8	2.0	1.4	6.7 ft	8	39 min
Gentle Breeze	3	7-10	8.5	1	0.6	1.0	1.2	0.8-5.0	3.4	2.4	20	9.8	17 hrs
			10	2	0.88	1.4	1.8	1.0-6.0	4	2.9	27	10	2.4
Moderate Breeze	4	11-16	12	2	1.4	2.2	2.8	1.0-7.0	4.8	3.4	40	18	3.8
			13.5	2	1.8	2.3	3.7	1.4-7.6	5.4	3.9	52	24	4.8
			14	3	2.0	3.5	4.2	1.5-7.8	5.6	4.0	59	28	5.2
			16	3	2.9	4.6	5.8	2.0-8.8	6.5	4.6	71	40	6.6
Fresh Breeze	5	17-21	18	4	3.8	6.1	7.8	2.5-10.0	7.2	5.1	90	55	8.3
			19	4	4.3	6.9	8.7	2.6-10.6	7.7	5.4	98	65	9.2
			20	5	5.0	8.0	10	3.0-11.1	8.1	5.7	111	75	10
Strong Breeze	6	22-27	22	5	6.4	10	13	3.4-12.2	8.9	6.3	134	100	12
			24	5	7.9	12	16	3.7-13.5	9.7	6.8	160	130	14
			24.5	6	8.2	13	17	3.8-13.6	9.9	7.0	164	140	15
			26	6	9.6	15	20	4.0-14.5	10.5	7.4	188	180	17
Moderate Gale[c]	7	28-33	28	6	11	19	23	4.5-15.5	11.3	7.9	212	230	20
			30	7	14	22	28	4.7-16.7	12.1	8.6	250	280	23
			30.5	7	14	23	29	4.8-17.0	12.4	8.7	258	290	24
			32	7	16	26	33	5.0-17.5	12.9	9.1	285	340	27
Fresh Gale	8	34-40	34	7	19	30	38	5.5-18.5	13.6	9.7	322	420	30
			36	7	21	35	44	5.8-19.7	14.5	10.3	363	500	34
			37	7	23	37	46.7	6-20.5	14.9	10.5	376	530	37
			38	7	25	40	50	6.2-20.8	15.4	10.7	392	600	38
			40	8	28	45	58	6.5-21.7	16.1	11.4	444	710	42
Strong Gale	9	41-47	42	8	31	50	64	7-23	17.0	12.0	492	830	47
			44	8	36	58	73	7-24.2	17.7	12.5	534	960	52
			46	9	40	64	81	7-25	18.6	13.1	590	1110	57
Whole Gale	10	48-55	48	9	44	71	90	7.5-26	19.4	13.8	650	1250	63
			50	9	49	78	99	7.5-27	20.2	14.3	700	1420	69
			51.5	9	52	83	106	8-28.2	20.6	14.7	736	1560	73
			52	9	54	87	110	8-28.5	21.0	14.8	750	1610	75
			54	9	59	95	121	8-29.6	21.8	15.4	810	1800	81
Storm	11	56-63	56	9	64	103	130	8.5-31	22.6	16.3	910	2100	88
			59.5	9	73	116	148	10-32	24	17.0	225	2500	101
Hurricane	12	64	64	9	80[b]	128[b]	164[b]	10-(35)	(26)	(18)			

[a] For hurricane winds (and often whole gale and storm winds) required durations and fetches are rarely attained. Seas are therefore not fully arisen.

[b] For such high winds, the seas are confused. The wave create blow off and the water and the air mix.

[c] A heavy box around this value means that the values tabulated are at the center of the Beaufort range.

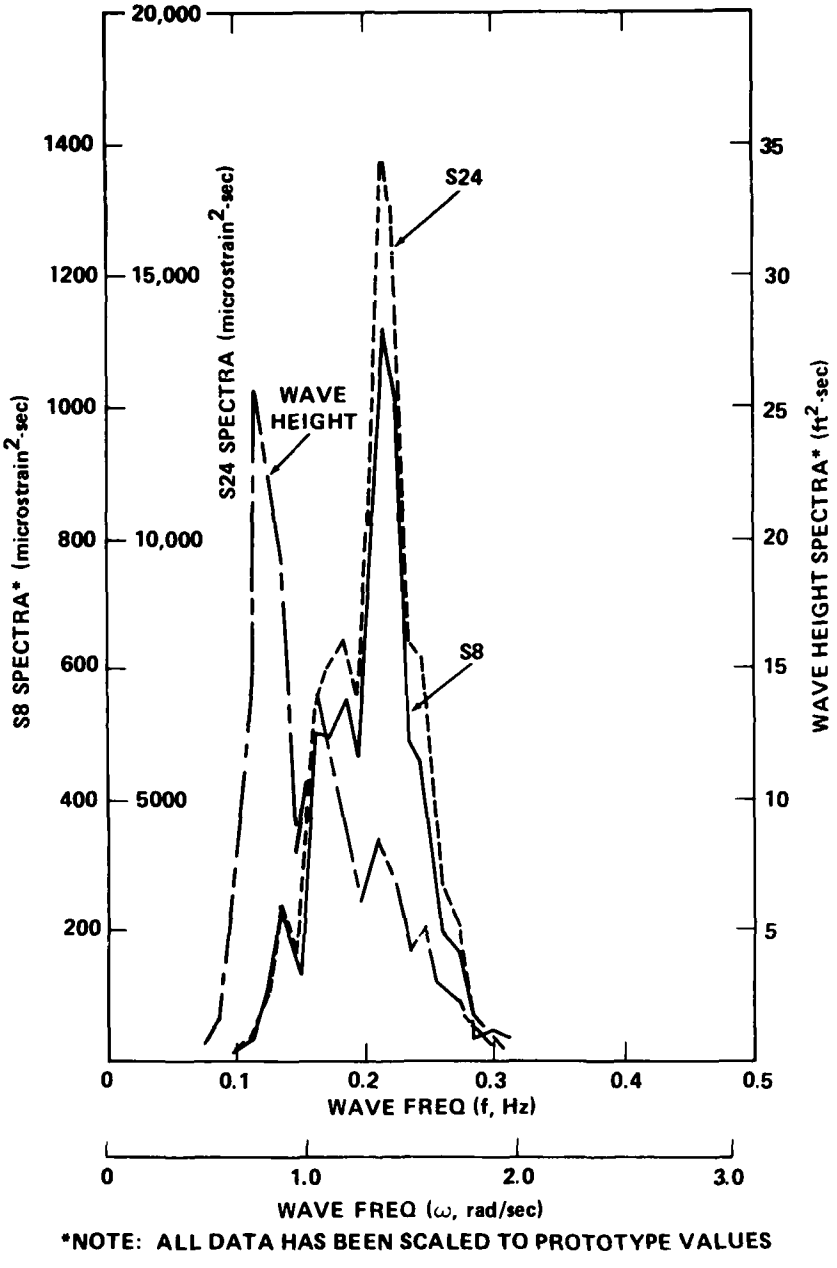

Figure 7 - Typical Model Response and Wave Height Spectra

A particularly useful aspect of spectral analysis is the determination of response amplitude operators (RAO's). As described by Andrews and Dinsenbacher,[4] RAO's characterize a response per unit of excitation and are obtainable from a knowledge of the excitation (waves) and the response (strain) spectra. RAO's were calculated for seven model primary strain bridges for low speed, beam seas (Figure 8).

Motion (roll, pitch, and heave) RAO's were determined for low speed, beam sea model data (Figure 9). A comparison of peak frequencies for the motion and strain RAO's shows that peak structural responses occur in much shorter waves than craft motions, indicating that structural responses are not strongly influenced by craft motion. A simple peak analysis of the model motion data for several headings was also performed; ratios were obtained of the average one-tenth highest ($H_{1/10}$) values of peak to peak motion per foot of $H_{1/10}$ peak to peak wave height. From these data, plots of motion characteristics were made for roll (Figure 10) and pitch (Figure 11). The data indicate that the most significant roll occurred during high speed stern quartering seas; pitch motion was worst during following seas for both low and high speed runs.

Wave Impact

Model wave impact pressure data were obtained from six pressure transducers installed as shown in Figure 2. Wave impacts on the model upper hull bottom were observed during several runs; the resulting data were analyzed to determine peak pressures for each heading, speed, and sea state combination. Figure 12 shows maximum measured point pressures as functions of run heading and transducer location. To facilitate comparisons with prototype impact data, model data shown in Figure 12 have been scaled to prototype values and drawn proportionally to the impact pressure magnitudes. Impact pressure data are plotted as a function of wave height in Figure 13; data have been scaled to the prototype. The figure includes data from two previous model tests as reported by Kallio and Davis[5] and Bedore.[6] A comparison of impact pressures for all three model tests shows good agreement. The plot indicates that pressure magnitudes for impacts in head and bow seas increase rapidly with wave height. More beam sea data are required for any trends to be observed with this heading. There is not sufficient data to accurately predict the effect of speed on pressure magnitude.

Figure 8 - Model Structural Response Amplitude Operators
for Low Speed, Beam Seas

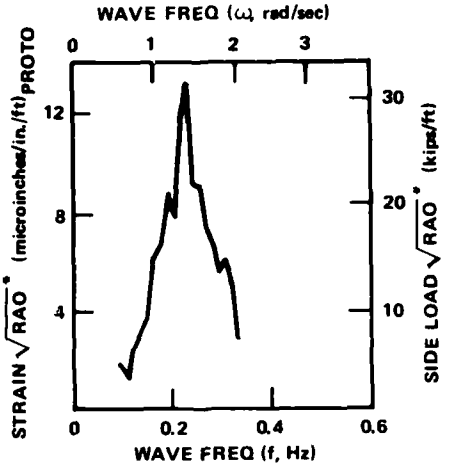

Figure 8a - S8 Forward Strut
Lateral Bending (Bulkhead E)

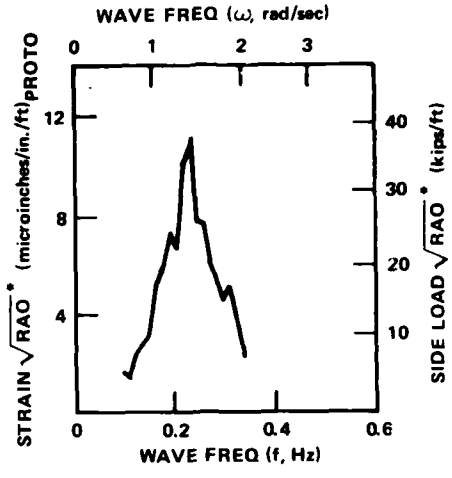

Figure 8b - S9 Forward Strut
Lateral Bending (Midchord)

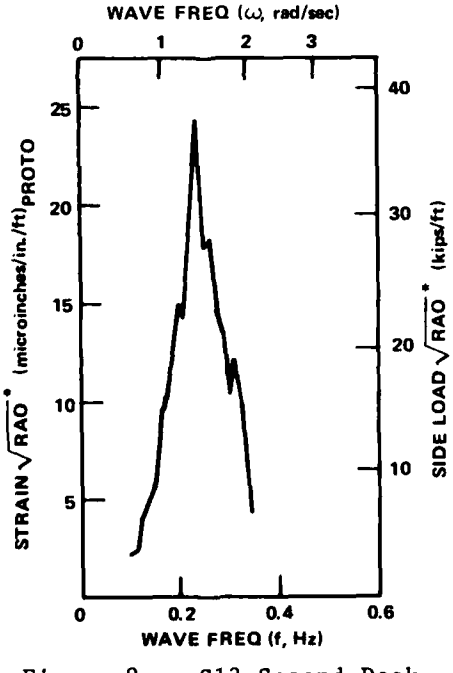

Figure 8c - S13 Second Deck
Bending Frame 17

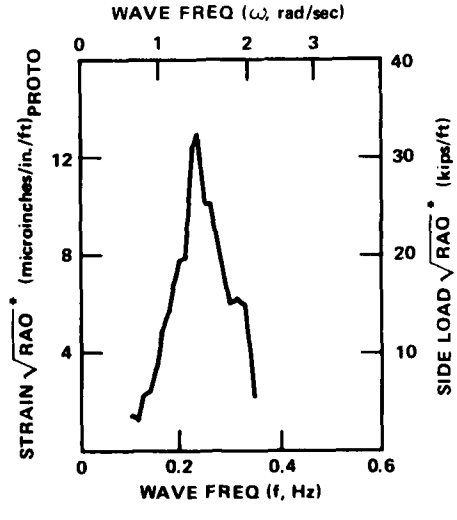

Figure 8d - S15 Main Deck
Bending Frame 17

*NOTE: ALL DATA HAS BEEN SCALED TO PROTOTYPE VALUES

Figure 8 (Continued)

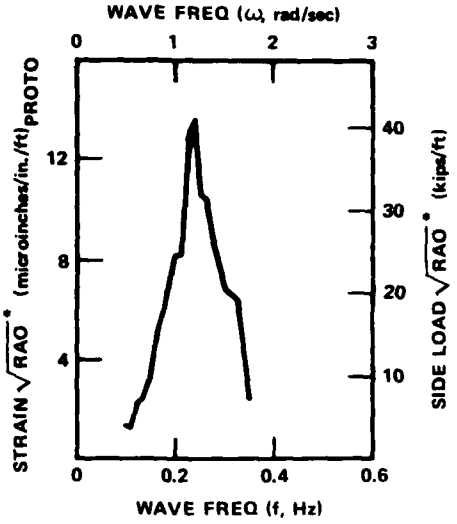

Figure 8e - S17 Main Deck Bending Bulkhead 13

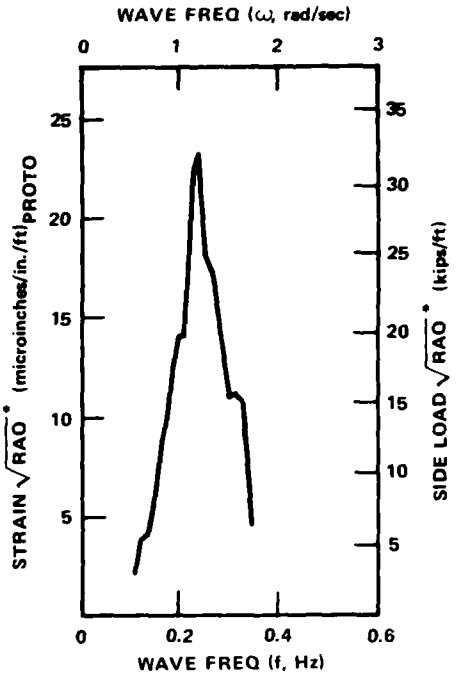

Figure 8f - S18 Second Deck Bending Bulkhead 13

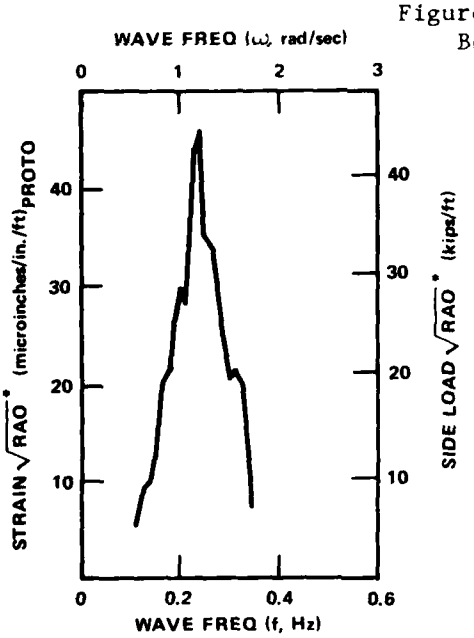

Figure 8g - S24 Diagonal Support Frame 19

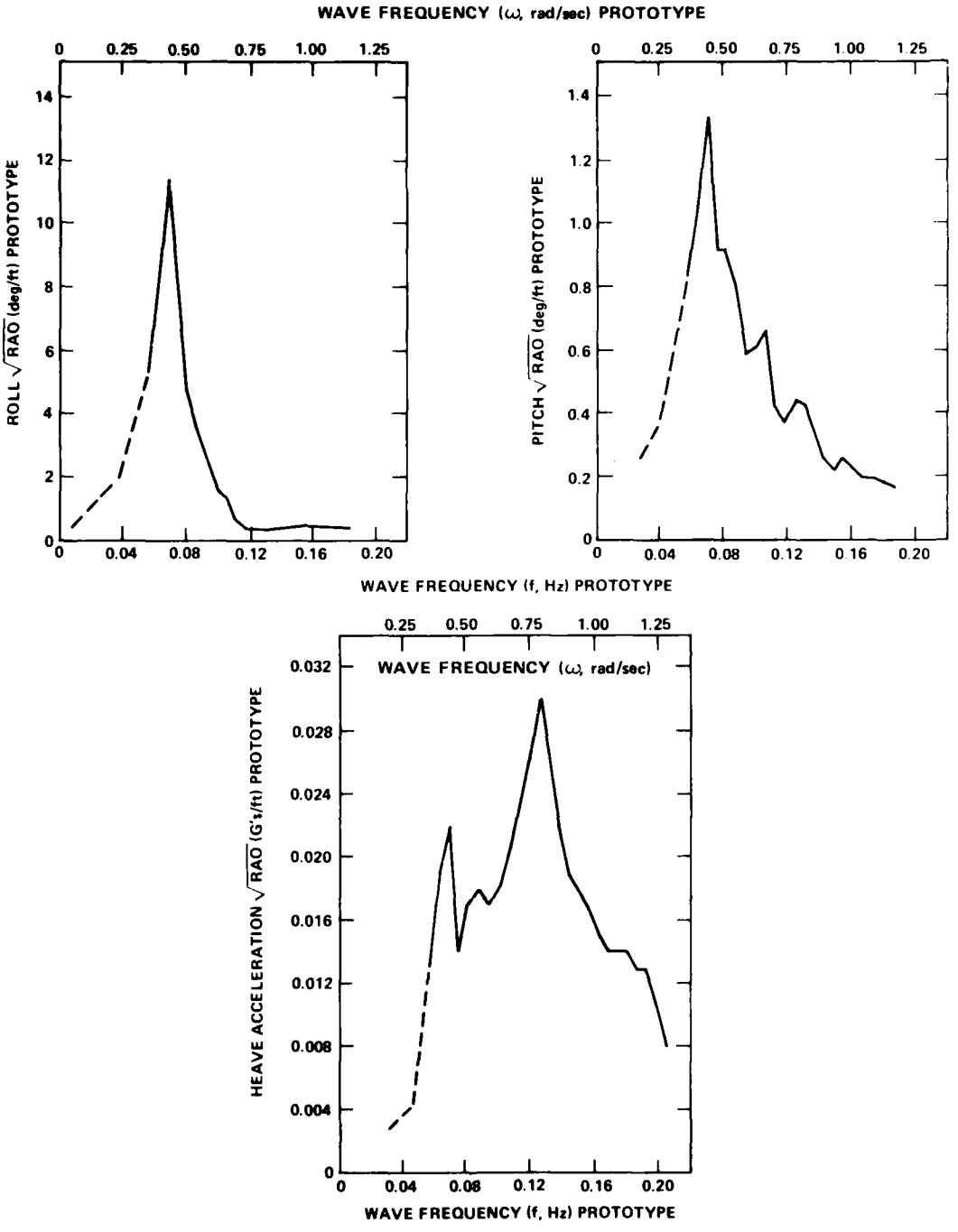

Figure 9 - Model Roll, Pitch, and Heave Acceleration Response Amplitude Operators for Low Speed, Beam Seas

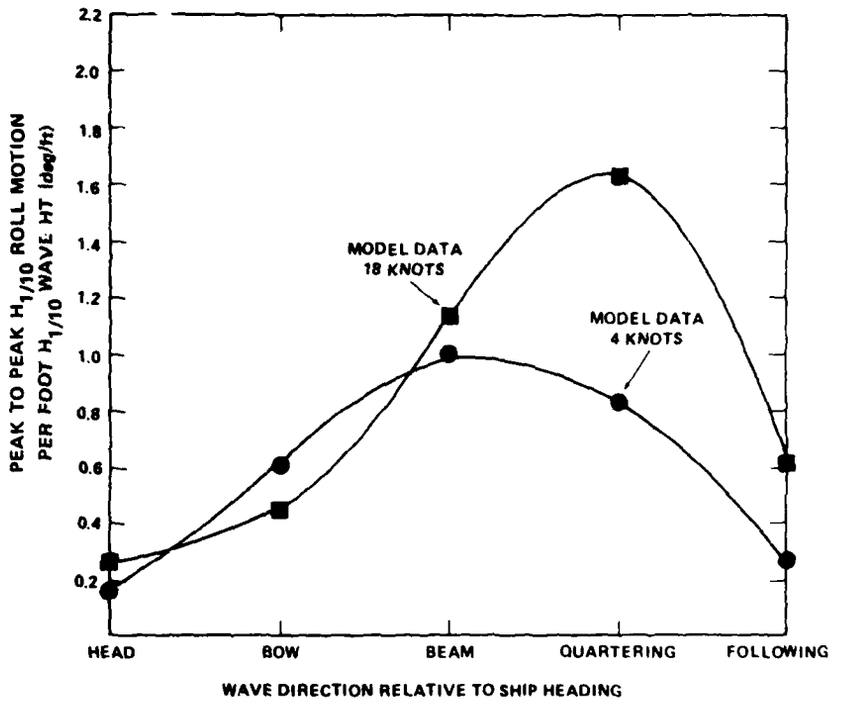

Figure 10 - Model Roll Characteristics

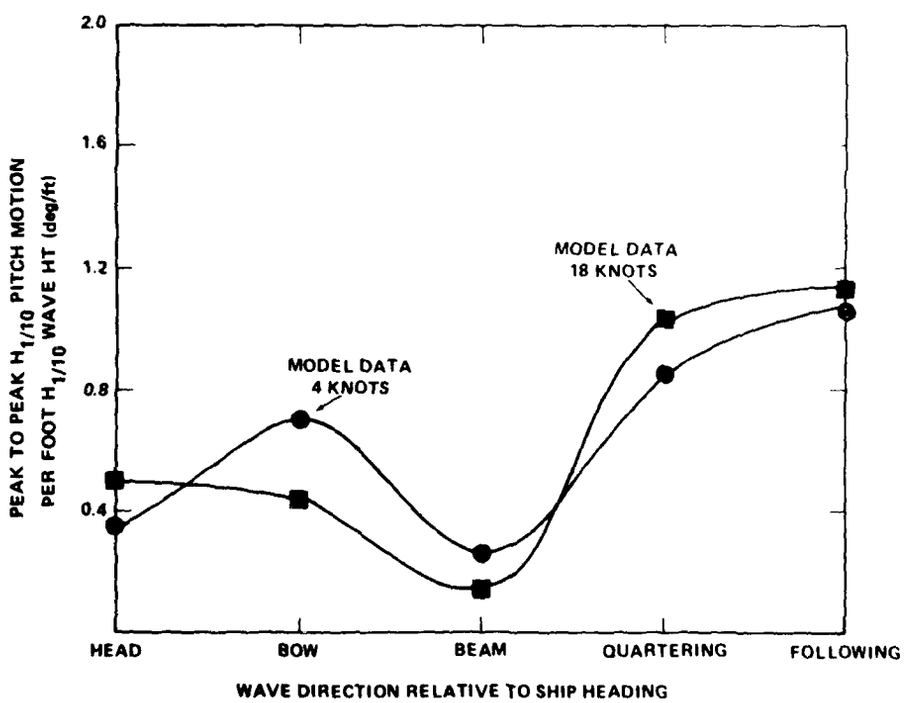

Figure 11 - Model Pitch Characteristics

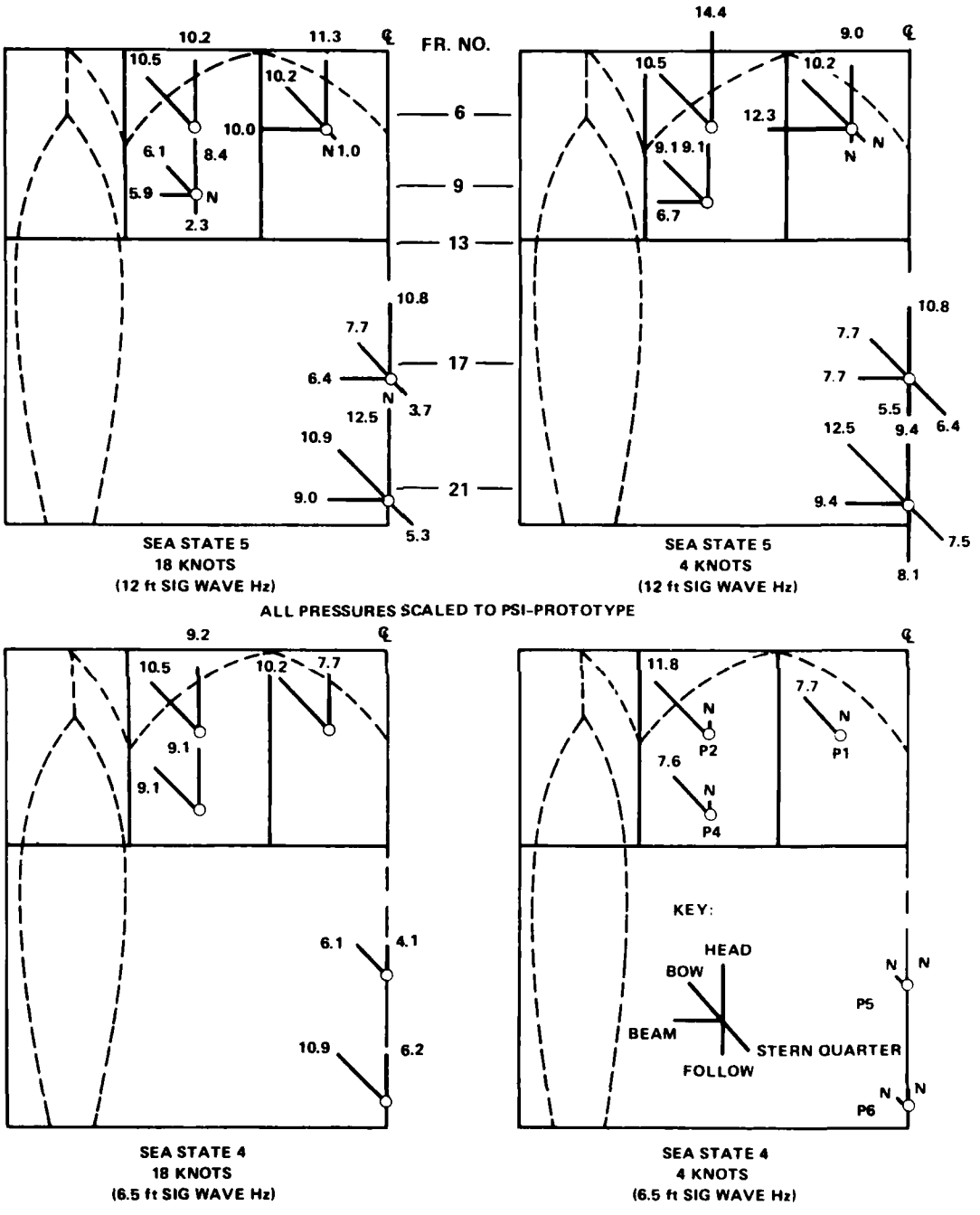

Figure 12 - Maximum Recorded Point Pressures for Model

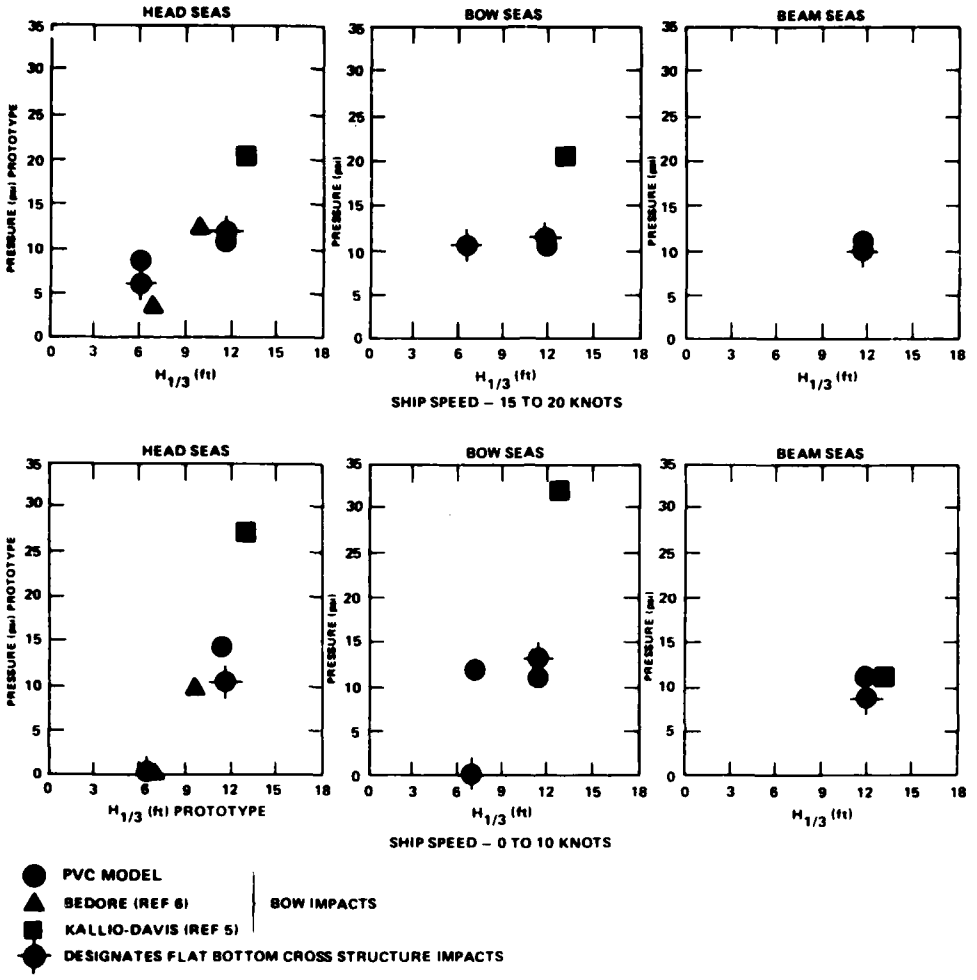

Figure 13 - Comparison of Maximum Impact Pressures for Three Stable Semi-Submerged Platform (SSP) Models

Using a simple strength of materials approach, possible wave impact structural deformation modes for the SSP prototype upper hull bottom plating and transverse stiffeners were calculated (Appendix C). Examination of the maximum impact pressures (Figures 12 and 13) indicates that pressures were measured on the model which, according to the calculations in Appendix C, would initiate yielding in the prototype bottom plating for sea conditions generally above Sea State 5. Yield initiation does not imply a high degree of structural deformation. It should be

noted that these impacts occurred during model runs with all control surfaces locked. Operational control surfaces may reduce the magnitude of the wave impacts; however, for design purposes and SSP operations the higher pressures should be considered due to the possibility of control surface failure.

PROTOTYPE TRIALS

Full-scale rough water trials on the SSP KAIMALINO were conducted in November 1976 off the northern coast of Oahu in the Hawaiian Islands; a summary of the structural trial runs is given in Table 8. Trial runs were a minimum of 15 minutes

TABLE 8 - SUMMARY OF PROTOTYPE TRIAL RUNS

KAIMALINO Run Number	Heading	Speed	Sea State
11-18-1	Port Beam	4 Knots	4
11-18-2	Following		
11-18-3	Head		
11-18-4	Port Beam		
11-18-5	Port Bow		
11-18-6	Port Beam		
11-26-1	Port Beam		5
11-26-2	Port Quartering		
11-26-3	Head		
11-26-4	Port Bow		
11-26-5	Port Beam		
11-26-6	Following		

duration with as little use made of the control surfaces during runs as possible. Wave height data for these trials were provided by the DTNSRDC Ship Performance Department Dutch Wave Rider Buoy which, prior to the initial run, was deployed from the SSP in the center of the trials area.

The SSP was modified by adding an inboard blister for increased buoyancy and fuel capacity on each lower hull prior to the performance of the full-scale trials. Although these blisters increased the craft displacement by approximately 25 tons,

they had little or no effect on the development of the loads data base. Because of mechanical problems with the port side engine during the trials, only the starboard engine was operating. While this resulted in an asymmetric thrust, rudder angle compensation required as a consequence was small due to the low craft speeds required for these trials.[7]

A preliminary peak analysis of the collected data determined which heading, relative to the seaway, produced the maximum responses. Figure 14 is a normalized plot of structural response per foot of wave height for two typical strain bridges The figure indicates that beam seas generated the maximum primary responses; thus a beam sea run, 11-26-1 (see Table 8), was selected for spectral analysis.

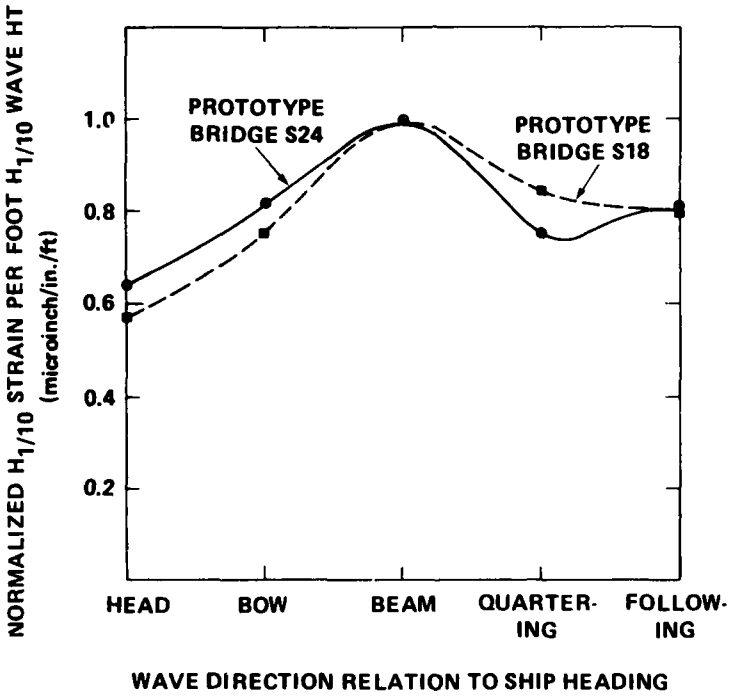

Figure 14 - Effect of Ship Heading on Normalized Prototype Structural Responses

Figure 15 gives selected prototype strain spectra and the corresponding measured wave height spectrum for low speed, beam seas. Using these structural response and wave height spectra, RAO's were determined for the SSP prototype strain bridges (Figure 16).

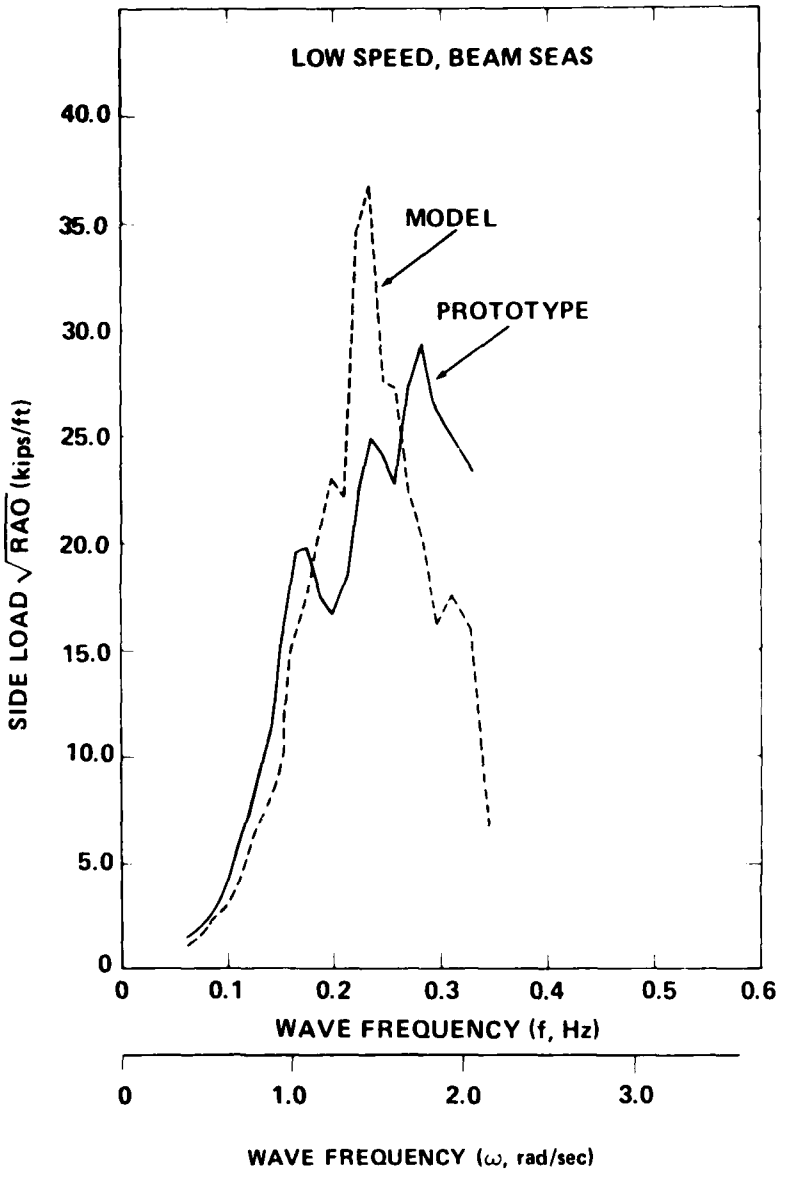

Figure 15 - Typical Prototype Response and Wave Height Spectra for Low Speed, Beam Seas

Figure 16 - Prototype Structural Response Amplitude Operators for Low Speed, Beam Seas

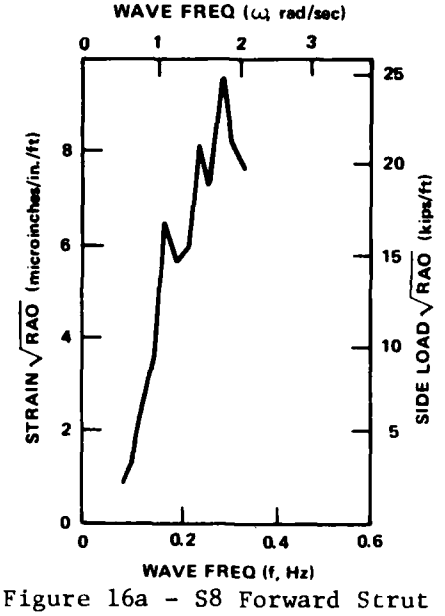

Figure 16a - S8 Forward Strut Lateral Bending (Bulkhead E)

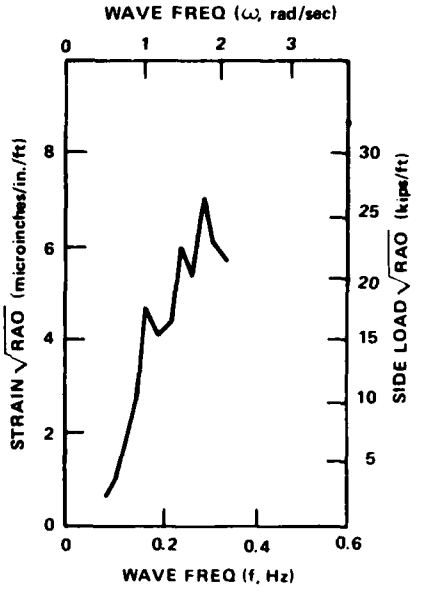

Figure 16b - S9 Forward Strut Lateral Bending (Midchord)

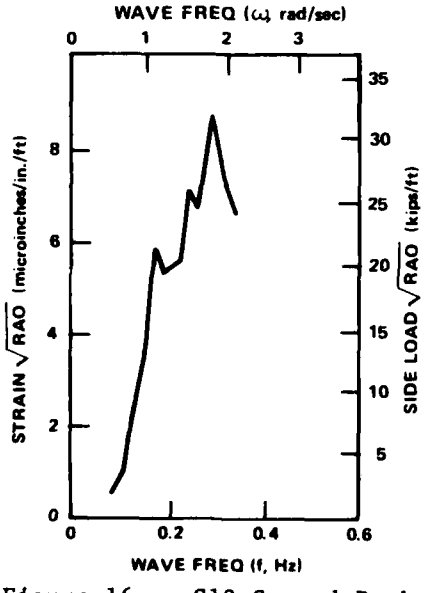

Figure 16c - S13 Second Deck Bending (Frame 17)

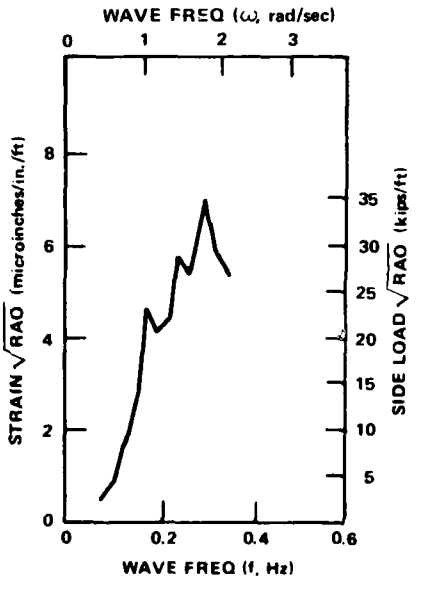

Figure 16d - S15 Main Deck Bending (Frame 17)

Figure 16 (Continued)

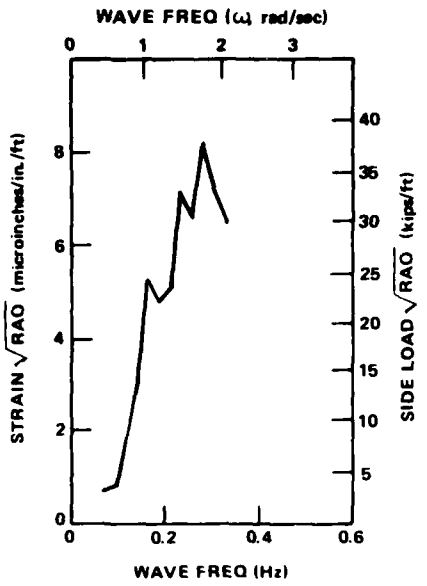

Figure 16e - S17 Main Deck Bending (Bulkhead 13)

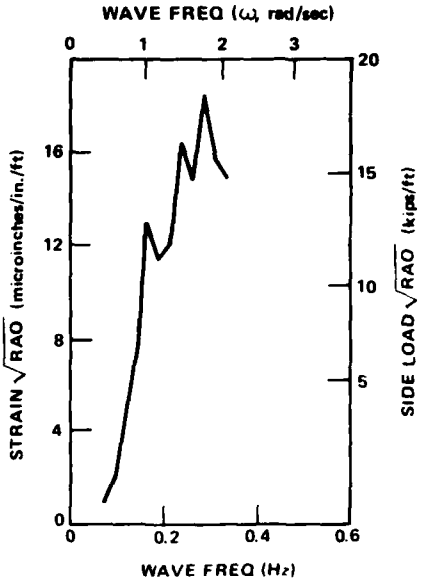

Figure 16f - S18 Second Deck Bending (Bulkhead 13)

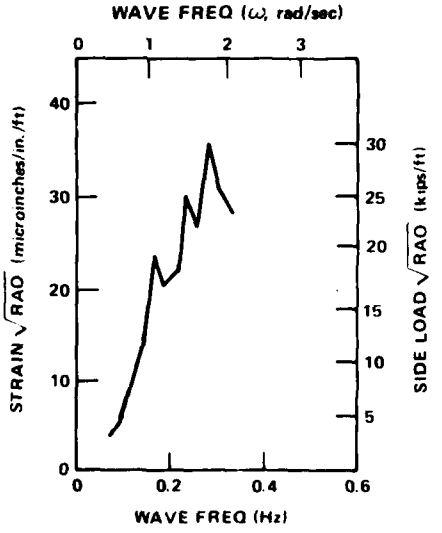

Figure 16g - S24 Diagonal Axial (Frame 19)

A comparison of prototype and model strains RAO's (Figures 8 and 16) indicates limited agreement. For the model, the frequency of the peak in the RAO is at 0.24 Hertz, corresponding to wavelengths of approximately 90 feet; for the prototype the frequency of the peak is 0.28 Hertz, corresponding to wavelengths of approximately 65 feet. A comparison between prototype and model strain data is as expected: vertical strut strain bridges agree well while upper hull strain bridges exhibit poor agreement, the result of scaling of the bow area in the model (described earlier).

Prototype wave impact data was collected by Ship Performance Department personnel during earlier full-scale trials. For these tests, 18 pressure transducers were installed along the upper hull bottom plating; Figure 17 gives their locations, as reported by Kallio.[8] Maximum point pressures, from transducers in locations corresponding to transducers on the model, are plotted in Figure 18 based on pressure magnitude and significant (average of the one-third highest peak-to-peak) wave height for speeds above and below the "hump" speed. Included in the figure are impact data obtained from the rigid vinyl structural model; a comparison of impact data trends between prototype and the model indicates good agreement.

SEA INDUCED LOADS DETERMINATION

SIDE LOADS

Simple sea induced loads data may readily be developed from detailed knowledge of test craft structural response to random waves and load sensitivity (i.e., load per unit measured strain). To facilitate comparison of prototype and model data and to permit predictions of side loads to be made for any given sea state, a side load RAO is the most useful form for presenting data. This side load RAO is calculated for each strain bridge by multiplying the magnitudes of the strain RAO's by the appropriate load/strain sensitivity.

Using this methodology, model load RAO's, have been calculated for each strain bridge and plotted (Figure 8--observe the right hand vertical axes). Based on these low speed, beam sea plots for the individual bridges a single mean value load RAO was calculated for the model (Figure 19). Comparison of the individual bridge RAO's with this mean value plot indicates agreement well within 20 percent; this is considered good from the perspective of experimental stress measurement and expected confidence bands in spectral analysis.

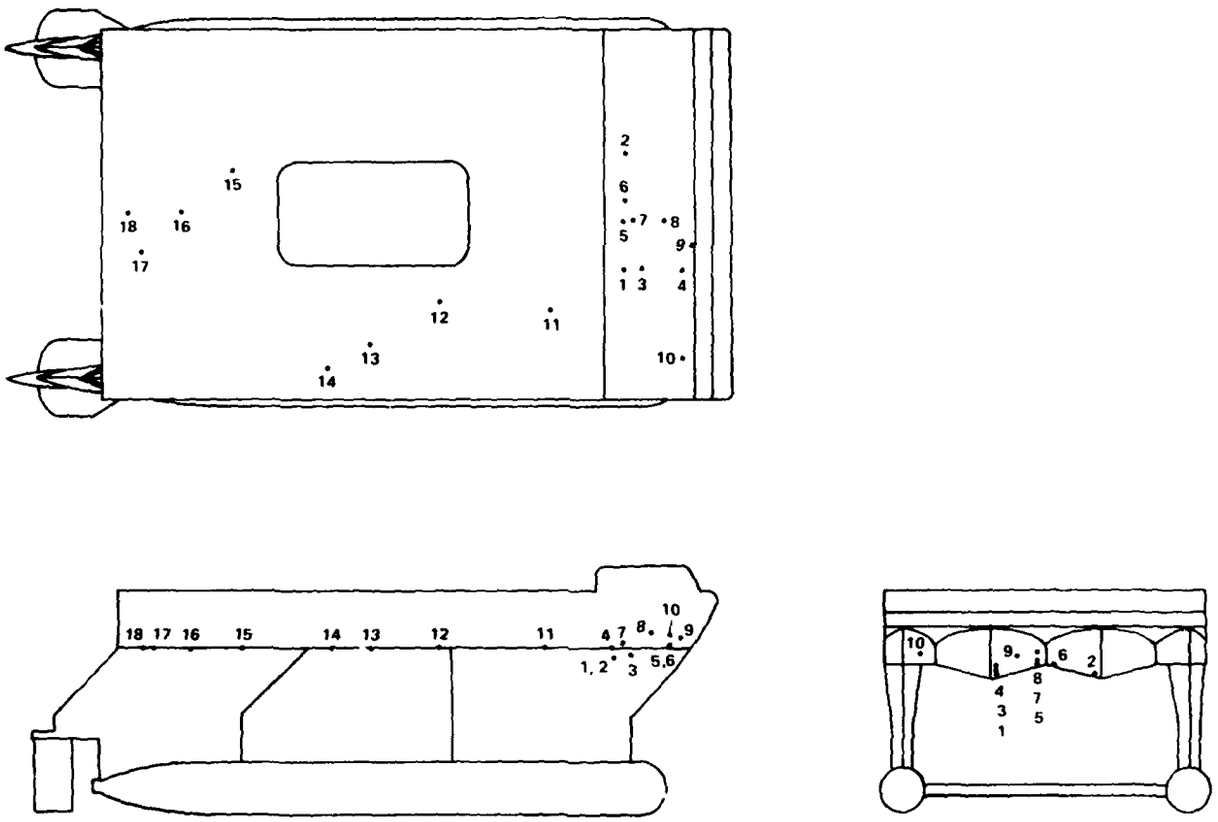

Figure 17 - KAIMALINO Prototype Pressure Gage Locations

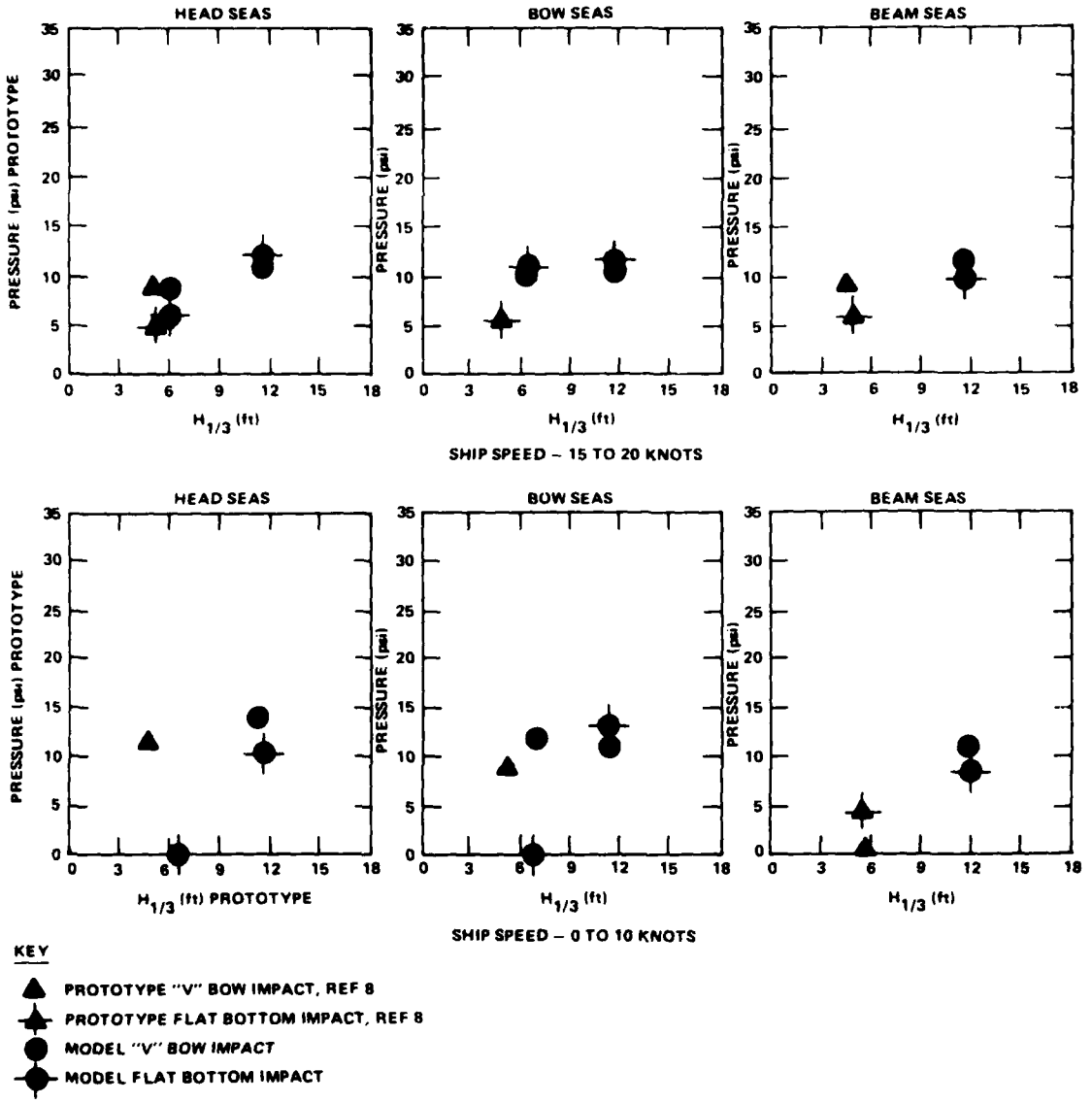

Figure 18 - Comparison of Maximum Impact Pressures for KAIMALINO Prototype and Model

Similarly, the prototype low speed, beam seas trials derived strain RAO's were multiplied by the appropriate load/strain sensitivities (Table 5) to produce a side load RAO for each prototype strain bridge. As Figure 16 shows the individual prototype strain bridge load RAO's are very consistent (note the right hand vertical axes). A mean value side load RAO was calculated for the prototype based on the individual plots (Figure 19).

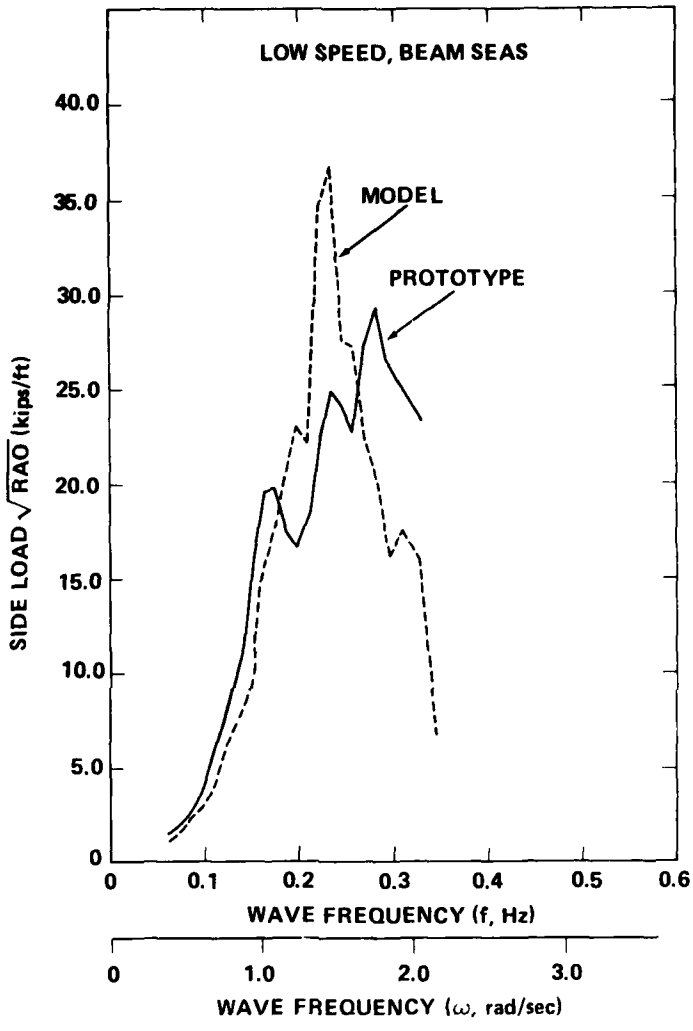

Figure 19 - KAIMALINO Prototype and Model Side Load Response Amplitude Operators for Low Speed, Beam Seas

A comparison of the empirically derived prototype and model side load RAO's in Figure 19 shows reasonably good agreement, particularly in the lower wave frequency band (corresponding to longer wavelengths). Figure 19 also shows that low speed, beam sea prototype and model side load RAO's peak in a band of frequencies corresponding to wavelengths approximately twice the waterline beam.

As discussed by Andrews and Dinsenbacher[3,4] an important property of a spectrum is that the area under the spectrum curve is related to the statistics of the original function, for example, the average, significant, and maximum values. Conversely, once a load spectrum has been generated for a particular sea state, estimates may be made of average, significant, or maximum side loads for that sea state. Since an RAO has been defined as the ratio of a response (or in this case, load) spectrum to a wave height spectrum, a load spectrum may be determined for any specific sea state by taking the product of the side load RAO, (Figure 19) and the appropriate wave height spectrum. Using the Pierson-Moskowitz sea spectra for Sea States 1 through 6 and the side load RAO's of Figure 19, prototype and model load spectra were separately calculated for Sea States 1 to 6 inclusive (see Table 7 for a description of the sea states). Estimates of significant sea-induced side loads, based on the enclosed areas of the calculated model and prototype load spectra for the range of sea states, have been plotted for low speed beam seas in Figure 20. The excellent agreement between prototype and model load estimates (Figure 20) validates the model as a load sensor. Secondary ordinate scales have been included in the figure to enable estimates to be made of structural responses for two key bridge locations: forward strut lateral bending (S8) and Frame 19 upper hull diagonal axial stress (S24). Maximum expected sea induced loads were also estimated based on the load RAO's of Figure 19 and the Pierson-Moskowitz sea spectra. Figure 21 gives plots of the maximum loads estimated from prototype and model data for craft operations in a Sea State 5--the SSP design condition. A comparison of these plots shows that estimates of prototype and model-based loads agree within five percent, thus validating the rigid vinyl/fiberglass model as a load sensor. The maximum load amplitude in Sea State 5 is estimated in Figure 21 at 0.4 of the craft displacement for 100 operational hours, and 0.5 of the craft displacement for 20 years of operation.

CONTROL SURFACE VERTICAL LOADS

To provide a data base on horizontal control surface loads, the load per unit strain sensitivities derived from the static loadings were applied directly to wave induced strain data. Maximum measured strains for representative runs were used to obtain simplistic estimates of maximum encountered seaway loads for a range of headings, speed, and sea conditions.

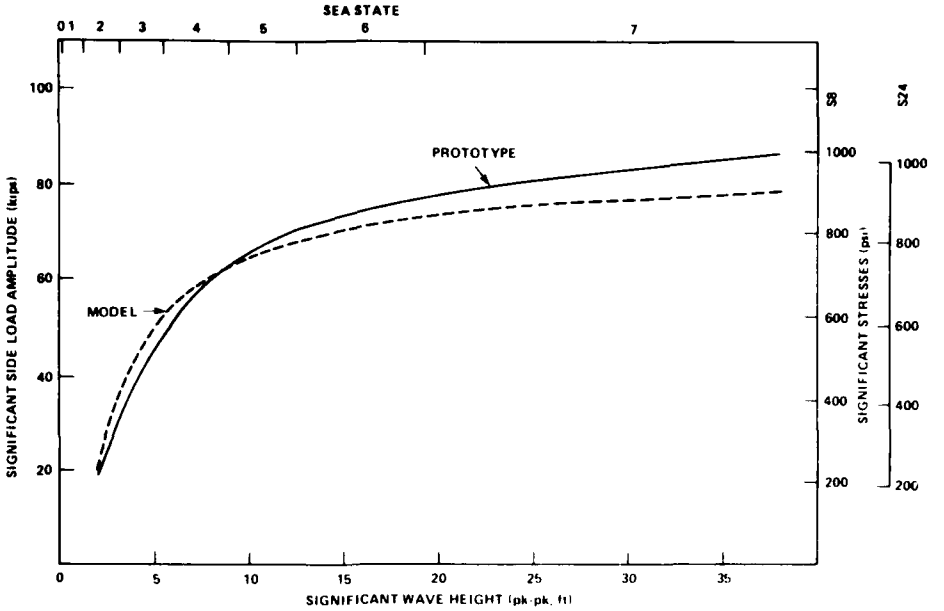

Figure 20 - Significant Side Load Estimates for Low Speed, Beam Seas

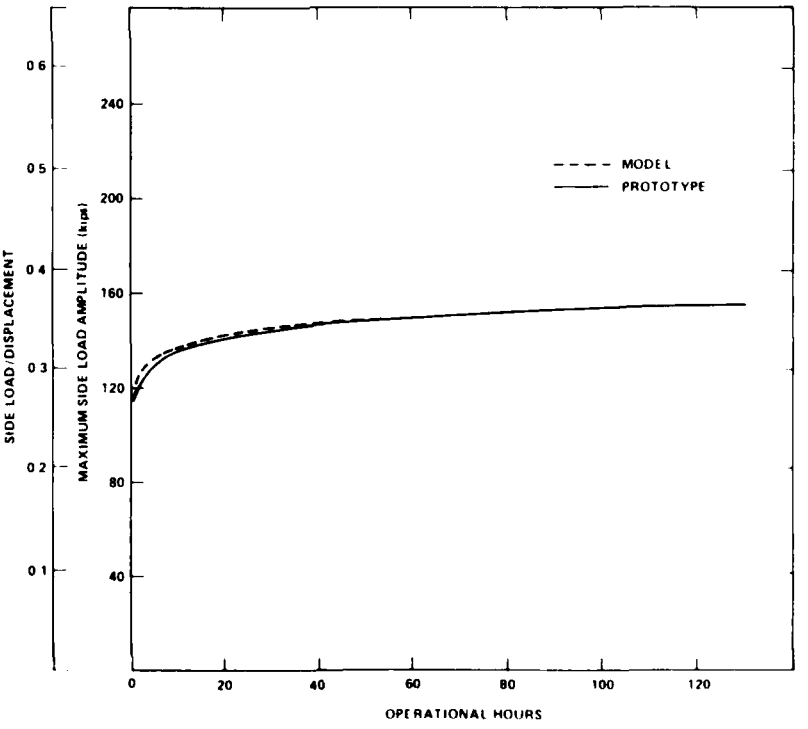

Figure 21 - Predictions of Maximum Side Load in Sea State 5 for KAIMALINO Prototype and Model

Prototype loads data for the canard are summarized in Table 9; Figure 22 is a plot of maximum canard load per foot of corresponding wave height. The data indicate that canard load is a maximum for head sea runs and, for the runs analyzed, is approximately 600 pounds (total peak to peak uniform load) per foot of wave height (peak to peak). Because of the limited data sample, and the canards being fixed during all runs, these estimated loads are, at best, rough approximations.

Loads for the aft stabilizer are based on model data and are summarized in Table 10 (the prototype gages were inoperable during sea trials). Maximum (peak to peak) stabilizer load was produced in stern quartering seas and is estimated at 11,900 pounds (total uniform full-scale load) per foot of wave height (peak to peak). Figure 23 gives plots of maximum load per foot of wave height as a function of ship heading relative to waves for speeds above and below "hump" speed. Because of the limited data, these values like those for the canard, are rough approximations.

TABLE 9 - SUMMARY OF KAIMALINO PROTOTYPE CANARD LOADS DATA

Heading	KAIMALINO Run No.	Stress (psi)	Uniform Load (kips)	Bending Moment (ft-lbs)	$\frac{\text{Load}}{\text{Wave Height}}$ (kips/ft)
Head	11-18-3	2700	7.68	21,800	0.62
↓	11-26-3	3700	10.51	29,800	0.60
Bow	11-18-5	1780	5.06	14,400	0.40
↓	11-26-4	2390	6.80	19,300	0.39
Beam	11-18-1	1460	4.15	11,800	0.36
	11-18-4	1680	4.78	13,600	0.37
	11-18-6	1440	4.09	11,600	0.33
	11-26-1	1630	4.62	13,100	0.27
	11-26-5	1540	4.36	12,400	0.27
Quarter	11-26-2	1270	3.60	10,200	0.21
Following	11-18-2	1510	4.28	12,100	0.34
↓	11-26-6	1400	3.98	11,300	0.23

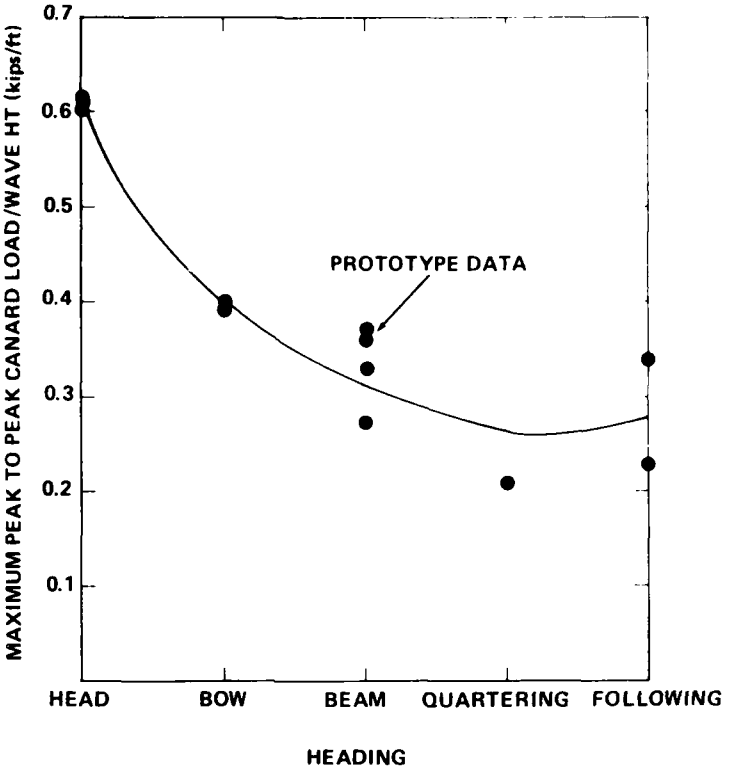

Figure 22 - Estimates of Canard Load for KAIMALINO Prototype

TABLE 10 - SUMMARY OF MODEL AFT STABILIZER LOADS DATA

Heading	Model Run No.	Speed (knots)	Sea State	Max Uniform Load (kips)	$\frac{\text{Load}}{\text{Wave Height}}$ (kips/ft)
Head	2	4	4	7.5	0.8
↓	7	18	4	22.6	3.1
	160	18	5	60.3	3.5
	162	4	5	24.5	1.0
Bow	33	4	4	22.9	1.7
↓	36	18	4	68.0	7.4
	47A	4	5	42.9	1.9
	53A	18	5	59.1	3.5
Beam	107	4	5	108.0	8.4
↓	120	18	5	187.9	9.6
Quarter	61	4	4	51.2	5.5
↓	78D	4	5	82.7	4.6
	80	18	5	104.7	11.9
Following	137	4	5	18.7	0.9
↓	139	18	5	20.9	3.2

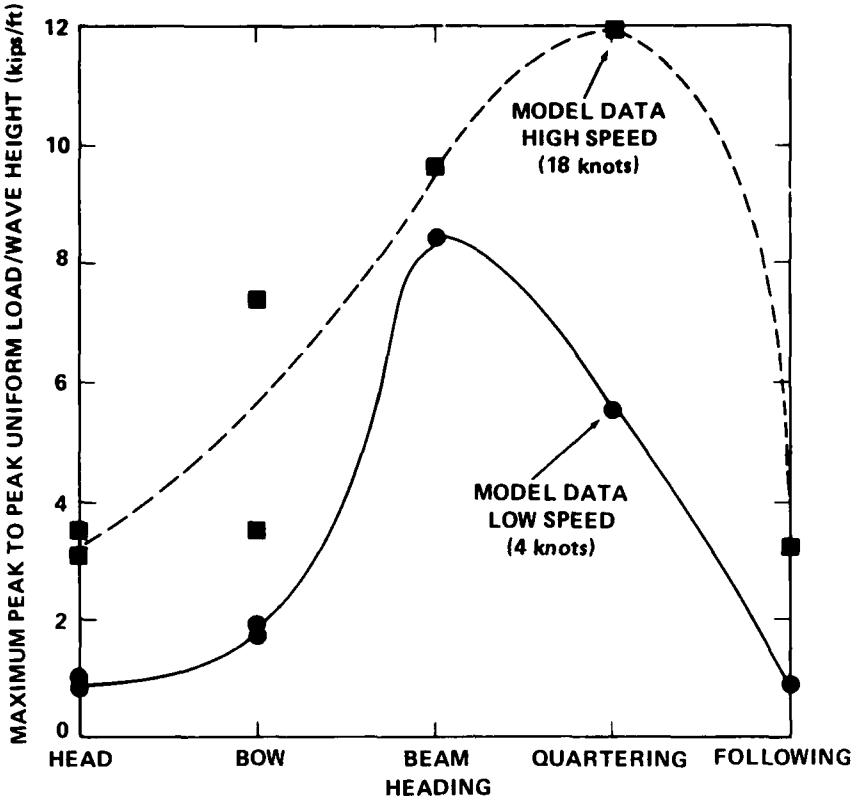

Figure 23 - Estimates of KAIMALINO Stabilizer Vertical Loads Based on Model Data

SUMMARY

A comprehensive test and evaluation of the SWATH prototype SSP KAIMALINO was essential for (1) improving current design loads criteria and (2) developing standards to minimize the structural weight fraction for future SWATH ship designs. The primary objective of the test program was to determine wave induced loads for the SSP KAIMALINO prototype and a scaled rigid vinyl/fiberglass model. A secondary objective was to evaluate rigid vinyl modeling of a complex structure as a design tool for obtaining strain responses and determining loads.

In acquiring sea induced loads data, it was necessary to determine load per unit strain sensitivities so that applied loads could be directly related to measured strains. The most reliable method for developing these load/strain sensitivities is to measure strain bridge response to known statically applied loads. This static load evaluation was performed on the prototype forward vertical

struts and on the horizontal control surfaces; scaled loadings were also performed on the model forward and aft struts and aft stabilizer.

The load sensitivities were applied to strain RAO's derived from sea trials to develop load RAO's based on both prototype and model data. Load spectra for several sea states were found by taking the products of the load RAO and the Pierson-Moskowitz sea spectra for the appropriate Sea States. From these load spectra, estimates were then made of significant side loads. Using model and prototype control surface static loading data and dynamic trials data simplistic estimates of control surface vertical loads were also made.

CONCLUSIONS

1. Available prototype and model data indicate that maximum primary wave induced side loads occur in beam seas. These maximum loads are estimated at one-half of the total displacement of the craft when extrapolated for operations in a Sea State 5 over a 20 year lifetime.

2. As indicated by the frequency of the peak in the beam sea structural response (strain) RAO and motion natural frequencies, structural responses are not strongly influenced by craft motion. The peak in the load RAO occurs for wavelengths approximately twice the waterline beam of the SSP while the peak in the roll RAO occurs in much longer waves.

3. As a load sensor the rigid vinyl model is excellent. Agreement of predictions for significant side loads based on model data is well within 10 percent of those based on prototype data.

4. Flotation blisters were installed on the lower hulls of the SSP prototype prior to the sea trials. The close agreement between model (with no blisters) and prototype data indicate that side load estimates were not influenced by the addition of the blisters.

5. The consistency of the side load RAO's derived from strain data of the seven primary bridges validates the method employed to derive sea induced loads, that is, by applying statically determined load per unit strain sensitivities to dynamic trials strain data.

6. The SSP KAIMALINO was an excellent candidate for static load calibration. Larger ships would have required larger loads to produce the same stress levels.

However, large ships are not proportionally stronger with respect to local structure. Therefore, many more load points and/or modifications to the local internal structure would have been required. This would have resulted in increased cost and ship downtime compared to the SSP static evaluation.

7. An evaluation of the model as a strain (or stress) sensor shows that the lower hull and forward strut strain response sensitivities agree well with corresponding prototype values. However, agreement of the model upper hull structural responses with prototype responses is considered poor; the lack of agreement may result from either or all of the following: scaling of the V-bow, shear lag effects due to distorted plating thickness employed in model scaling; out-of-flat plating in the prototype. It should be noted that the discrepancy is consistent and therefore correctable.

8. With respect to wave impact, model tests indicate that the most severe operating conditions are higher speed, head and bow sea headings in a Sea State 5 and above.

9. During high Sea State 5 model tests, wave impact pressures were measured which, according to simple strength of materials calculations, are estimated to initiate yielding in the prototype upper hull bottom plating (yield initiation does not imply severe structural deformation). Although the impacts occurred with control surfaces locked, these magnitudes should be considered due to the possibility of control surface failure on the prototype.

10. Prototype wave impact data trends obtained during Sea State 3 to 4 operations agree well with corresponding data trends from the rigid vinyl structural model.

11. As determined from the prototype aft stabilizer static loading, the stabilizer-lower hull end connection acts 67 percent fixed. Based on a similar scaled static evaluation of the model aft stabilizer, the model end connection was determined to act 59 percent fixed. Using these end fixities, relationships between total uniform load and stabilizer vertical bending strains were derived. For the prototype this ratio was calculated at 1047 pounds per microstrain; for the model the ratio was determined to be 1100 pounds per microstrain. The agreement, well within ten percent, is considered excellent from the perspective of experimental measurements.

12. The aft stabilizer natural frequency in water was calculated at 6.8 Hz.

13. The maximum aft stabilizer load (peak to peak) recorded was 11.9 kips/ft wave height (crest to trough) for higher speed stern quartering seas

14. The maximum recorded canard vertical load (peak to peak) was 10.5 kips (equivalent to 0.6 kips/ft wave height) for head seas with canards fixed.

ACKNOWLEDGMENTS

The SSP structural test program comprised two major efforts: model design, construction, testing, and data analysis; and prototype planning, instrumenting, testing, and data analysis. During both phases of the program Mr. A. Dinsenbacher played a key role in obtaining funding and actively guiding the overall effort.

In addition, the author appreciates the work of the following individuals: Messrs. J. Rodd, S. Austin, and G. Lauver who were responsible for the construction and testing of the model and Messrs. R. Swanek and H. Ford who aided in analysis of the model data.

The success of the prototype trials effort was due directly to the excellence and cooperation of the NOSC detachment at Kaneohe Bay, Hawaii, especially T. Hughes and the SSP KAIMALINO crew. The expertise of the DTNSRDC test crew consisting of Messrs. G. Elmer, E. Wolfe, R. Stenson, G. Minard, D. Huminik, J. Kallio, J. Fein, and particulary co-worker J. Hardison, also played an important role. During SSP construction the help and cooperation of Mr. T. Strickland of NOSC and Lt. J. Payne of the Curtis Bay Coast Guard Yard was greatly appreciated.

Additional personnel involved during various phases of the program and deserving credit are: Messrs. K. Spates, J. Birmingham, W. Mosedale, H. Brisker, D. Ricks, R. Busby, G. Toms, F. Palmer, J. Berkley, and P. Branch.

Valuable comments made by Messrs. A. Dinsenbacher, N. Nappi, and Dr. M. Critchfield who reviewed this report are also appreciated.

APPENDIX A

SSP STABILIZER DATA ANALYSIS

GENERAL DERIVATION

The simplified beam of Figure A.1 represents the SSP KAIMALINO stabilizer and its connection to the lower hulls. The loads shown in the figure represent any pair of symmetrically applied concentrated loads. By superposition (Figure A.1), this is equivalent to a simply supported beam plus a pair of end moments representing the unknown moments developed by the torsional spring supports.

The total rotation of the beam at its supports, θ, is the sum of the rotation caused by the concentrated load, θ_p, and the end moments, θ_m:

$$\theta = \theta_p + \theta_m$$

From standard strength of materials

$$\theta_p = \frac{Pd}{4EI} (L-d)$$

and,

$$\theta_m = \frac{M_e L}{2EI}$$

Define a spring constant, K, such that:

$$M_e = -K\theta \tag{A.1}$$

Then,

$$\theta = \theta_p + \theta_m = \frac{Pd}{4EI} (L-d) - \frac{K\theta L}{2EI}$$

or,

$$\theta = \frac{Pd(L-d)}{4EI\left(1+ \frac{KL}{2EI}\right)} \tag{A.2}$$

If the beam were fixed, then:

$$(M_e)_{FIXED} = \frac{Pd(L-d)}{2L} \tag{A.3}$$

The ratio of the actual end moment to the moment for a fixed end beam using Equations (A.1) through (A.3) is as follows:

$$\frac{M_e}{(M_e)_{FIX}} = \frac{K\theta}{(M_e)_{FIX}} = \frac{\frac{PdK(L-d)}{4EI\left(1+\frac{KL}{2EI}\right)}}{\frac{Pd(L-d)}{2L}}$$

Defining R as the following ratio:

$$R = \frac{M_e}{(M_e)_{FIX}} \tag{A.4}$$

Then,

$$R = \frac{KL}{2EI + KL} = \frac{1}{\frac{2EI}{KL} + 1} \tag{A.5}$$

Note that as R is a function of only relative stiffness of the beam and support, it is independent of the dimension d. Since any symmetric load may be expressed as a sum of pairs of symmetric concentrated loads, Equation (A.5) holds even for uniformly distributed loads.

The prototype static stabilizer evaluation consisted of two vertical loadings applied at two locations on either side of the craft centerline. Strain gage bridges at three locations were monitored to obtain bending moments at midspan and 14 inches from either end connection (Figure A.2). Both moments M_o and M_1 are based on measured strains. As a result of symmetry about the centerline, the vertical shear in the stabilizer is P/2; therefore:

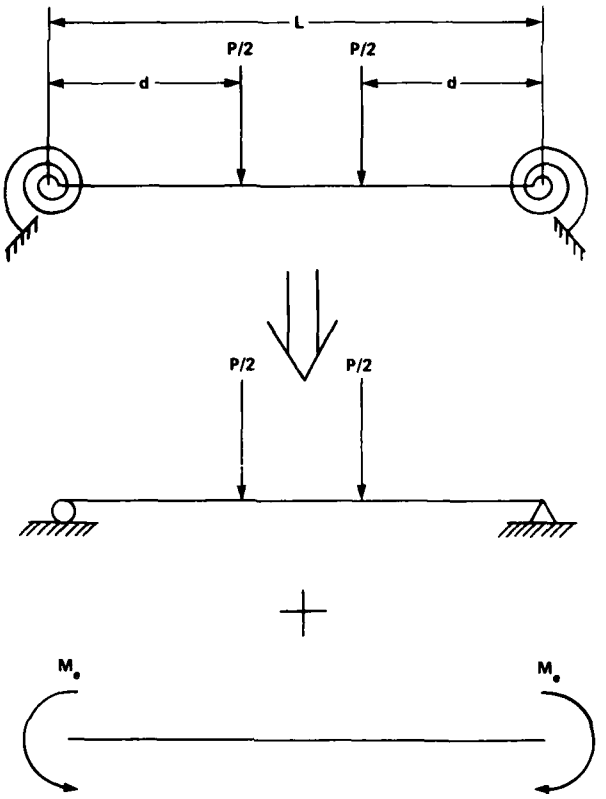

Figure A.1 - Beam Diagram--Stabilizer

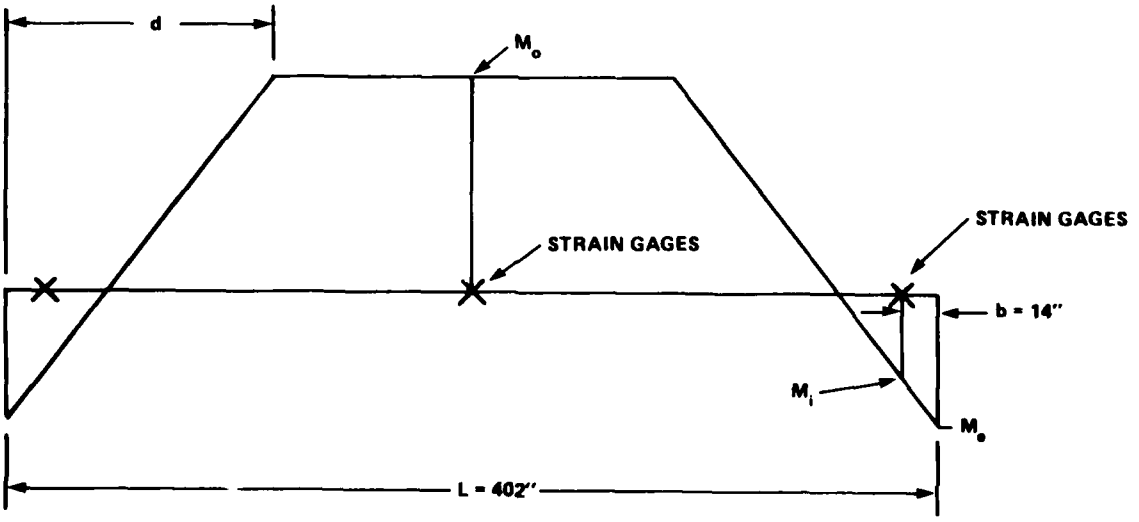

Figure A.2 - Stabilizer Moment Diagram

$$M_e = M_1 + \left(\frac{P}{2}\right)(b) \qquad (A.6)$$

from Equation (A.3)

$$(M_e)_{FIX} = \frac{Pd(L-d)}{2L}$$

and

$$\left(\frac{P}{2}\right)(d-b) = M_o + M_1$$

or,

$$P = \frac{2(M_o+M_1)}{(d-b)}$$

therefore:

$$R = \frac{M_1 + \left(\frac{Pb}{2}\right)}{\frac{Pd(L-d)}{2L}} \qquad (A.7)$$

Substituting for P we get

$$R = \frac{M_1 + b\left(\frac{M_o+M_1}{d-b}\right)}{\frac{(M_o+M_1)(d)(L-d)}{(d-b)(L)}}$$

Simplifying:

$$R = \frac{\left(\frac{d}{L}\right) + \left(\frac{M_o}{M_1}\right)\left(\frac{b}{L}\right)}{\left(\frac{d}{L}\right)\left(1+ \frac{M_o}{M_1}\right)\left(1- \frac{d}{L}\right)}$$

Thus R is expressed as a function of nondimensional ratios of geometry and experimentally measured moments. These moments may be derived from measured strain data, using the following relationships:

$$M_o = \frac{EI\varepsilon_o}{C_o} \text{ and } M_1 = \frac{EI\varepsilon_1}{C_1}$$

where,

$$\frac{M_o}{M_1} = \left(\frac{EI\varepsilon_o}{EI\varepsilon_1}\right)\left(\frac{C_1}{C_o}\right) = \left(\frac{C_1}{C_o}\right)\left(\frac{\varepsilon_o}{\varepsilon_1}\right)$$

Therefore:

$$R = \frac{\left(\frac{d}{L}\right) + \left(\frac{C_1}{C_o}\right)\left(\frac{\varepsilon_o}{\varepsilon_1}\right)\left(\frac{b}{L}\right)}{\left(\frac{d}{L}\right)\left[\left(\frac{C_1}{C_o}\right)\left(\frac{\varepsilon_o}{\varepsilon_1}\right)+1\right]\left(1- \frac{d}{L}\right)} \qquad (A.8)$$

PROTOTYPE

Figure A.3 is a cross section of the SSP prototype stabilizer. Using the results of the two static loadings, the stabilizer end fixity R is calculated from Equation (A.8).

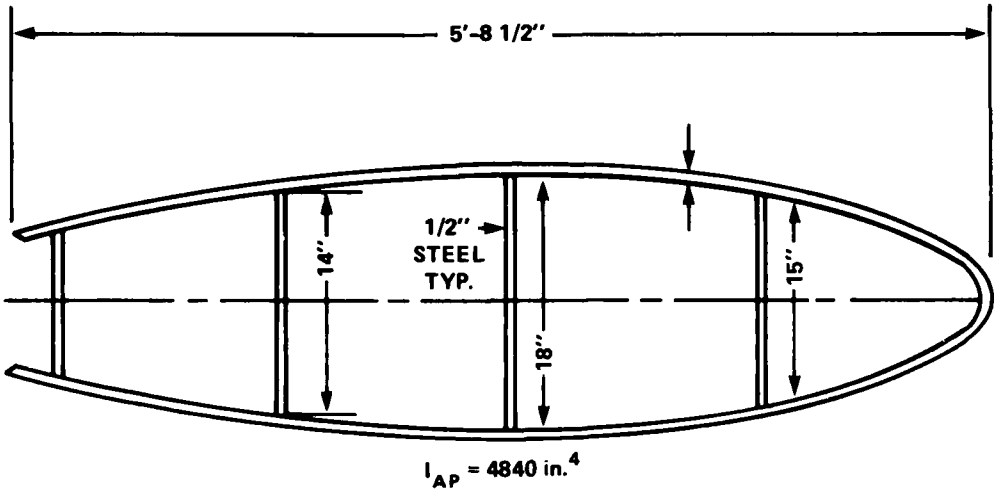

Figure A.3a - Prototype Stabilizer

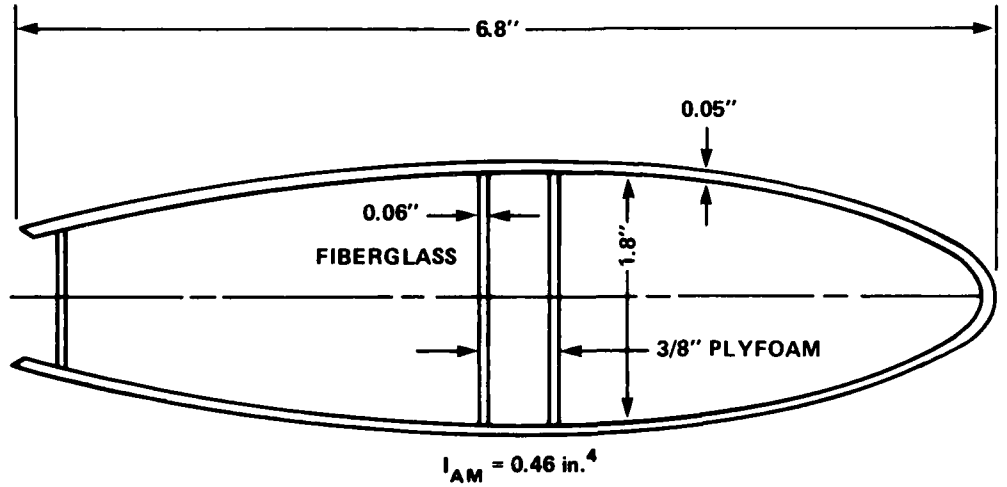

Figure A.3b - Model Stabilizer

Figure A.3 - KAIMALINO Aft Stabilizer Cross Section

"Center" Load (15 3/4 inches either side of craft centerline)

$b = 14$ in. $\quad \varepsilon_o = 63$ μin./in. $\quad C_o = 8$ in.

$d = 185.3$ in. $\quad \varepsilon_1 = 32$ μin./in.

$L = 402$ in. $\quad C_1 = 9$ in.

$$R = \frac{(0.46) + (1.125)(1.97)(0.035)}{(0.46)[(1.125)(1.97)+1](0.54)} = 0.673$$

"Outer" Load (87 inches either side of centerline)

$b = 14$ in. $\quad \varepsilon_o = 34$ μin./in. $\quad C_o = 8$ in.

$d = 113.3$ in. $\quad \varepsilon_1 = 26$ μin./in.

$L = 402$ in. $\quad C_1 = 9$ in.

$$R = \frac{(0.28) + (1.125)(1.308)(0.035)}{(0.28)[(1.125)(1.308)+1](0.72)} = 0.665$$

The agreement between the two calculated values of R is considered very good for experimental results. An average value $\overline{R}$ is used in further calculations:

$$\overline{R} = 0.669 = 66.9 \text{ percent}$$

As a check, this value of $\overline{R}$, which was determined only from ratios of geometry and experimental data, was to back-calculate "predicted" values of strain. Using:

$$\varepsilon_1 = \frac{M_1 C_1}{EI}$$

where

$$M_1 = M_e - \left(\frac{P}{2}\right)(b) = (M_e)_{FIX}(\overline{R}) - \left(\frac{P}{2}\right)(b) \qquad (A.9)$$

and

$$\epsilon_o = \frac{M_o C_o}{EI}$$

where

$$M_o = \left(\frac{P}{2}\right)(d-b) - M_1$$

Then, from Figure A.3

$$I_{proto} = 4840 \text{ in.}^4$$

strains were calculated and are compared with measured strains. Table A.1 shows that calculated strains are consistent with measured strains, thus verifying the reliability and accuracy of the field experiments.

With the end fixity known, it is relatively simple to determine the end moment for any symmetric load, including uniform loads.

$$M_e = \bar{R}(M_e)_{FIXED} = \frac{\bar{R}WL}{12}$$

where W is the total uniform load.
Therefore:

$$W = \frac{12M_e}{\bar{R}L} \qquad \text{(A.10)}$$

From Equation A.9:

$$M_e = M_1 + \frac{Wb}{2} \text{ and } M_1 = \frac{EI\epsilon_1}{C_1}$$

TABLE A.1 - COMPARISON OF ESTIMATED AND MEASURED STRAINS FOR STABILIZER EVALUATION

Strain Bridge	Load and Location	Structural Responses (μin./in.)		Percent Error
		Calculated	Measured	
ε_1	20,000 lb @ 15 in.	33	32	3
ε_o	20,000 lb @ 15 in.	65	63	4
ε_1	20,000 lb @ 87 in.	25	26	3
ε_o	20,000 lb @ 87 in.	33	34	4

Equation (A.10) becomes:

$$W = \frac{-12EI\varepsilon_1}{C_1(\bar{R}L-6b)} \tag{A.11}$$

For the SSP prototype Equation (A.11) becomes:

$$W = (1047\times10^6)(\varepsilon_1) \tag{A.12}$$

Substituting

$$M_e = -M_o + \frac{WL}{8} \text{ and } M_o = \frac{EI\varepsilon_o}{C_o}$$

Equation (A.10) now becomes:

$$W = \frac{-12EI\varepsilon_o}{C_oL\left(\bar{R}-\frac{3}{2}\right)} \tag{A.13}$$

For the SSP prototype Equation (A.13) becomes:

$$W = (652\times10^6)(\varepsilon_o) \tag{A.14}$$

These relationships are plotted as Figure A.4.

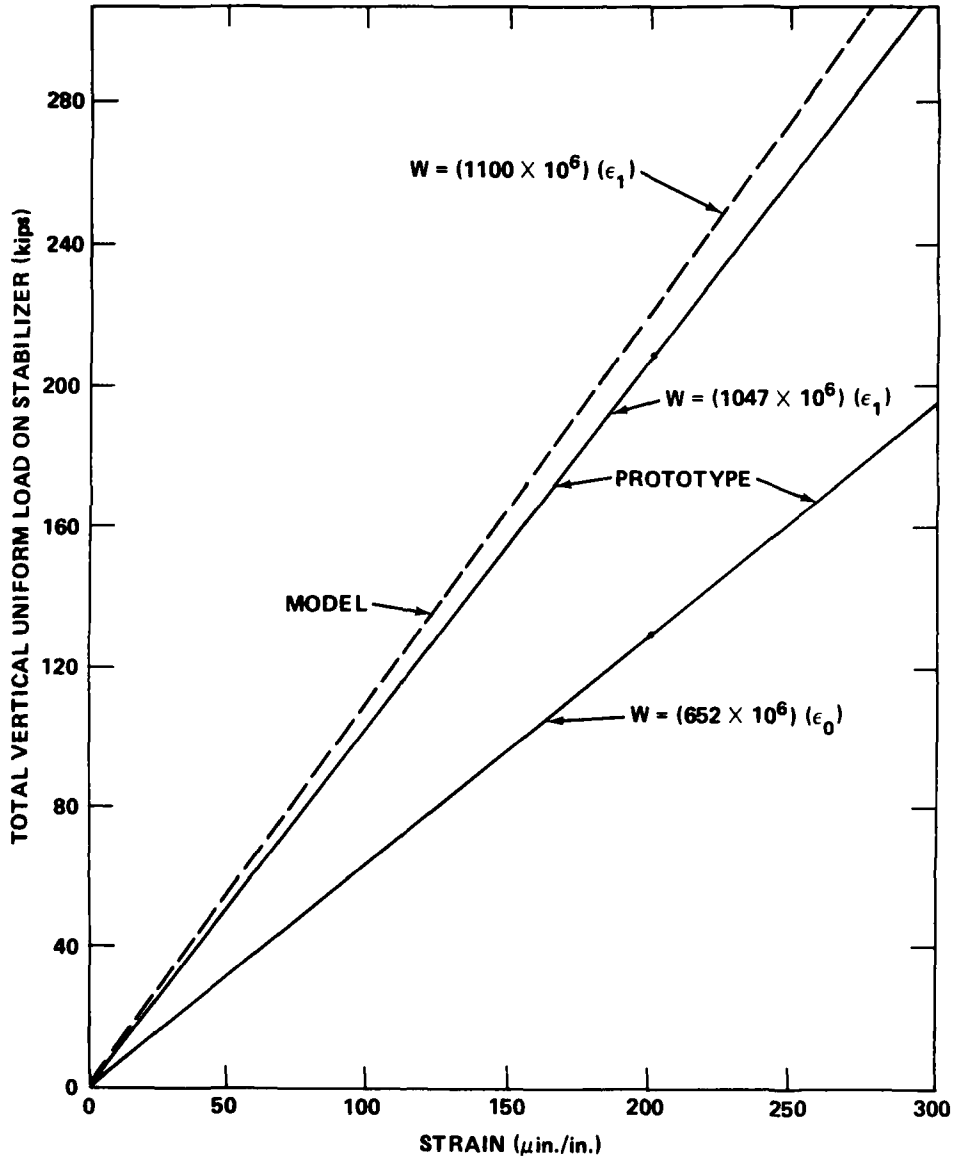

Figure A.4 - Estimates of Total Vertical Load on KAIMALINO Aft Stabilizer from Strain Bridge Data

MODEL

A cross section of the model aft stabilizer is shown in Figure A.3; note that the three prototype transverse vertical stiffeners have been scaled to a single stiffener in the model. Because commercially available thicknesses of plastic and fiberglass were used for model construction, the area moments of inertia did not scale exactly as λ^4. For the aft stabilizer, this difference is approximately four percent.

For the model stabilizer evaluation, only the end connection strain bridges were operational. Using these measured strains, end fixity is calculated from Equation (A.7):

$$R = \frac{M_1 + \left(\frac{P}{2}\right)(b)}{\frac{Pd(L-d)}{2L}} = \frac{(2EI\varepsilon+Pbc)L}{Pdc_1(L-d)}$$

Where $E = 3 \times 10^6$ psi, $I = 0.46$ in.^{4}, $\varepsilon = 24 \times 10^{-6}$ in./in., $P = 17.7$ lb, $b = 1.4$ in., $d = 14.1$ in., $c = 0.85$ in., $L = 40.2$ in.

or,

$$R_m = \frac{[(2)(3\times10^6)(0.46)(24\times10^{-6}) + (17.7)(1.4)(0.85)](40.2)}{(17.7)(14.1)(0.85)(40.2-14.1)}$$

$$R_m = 0.59$$

The model stabilizer end fixity is calculated to be 59 percent fixed, which agrees well with prototype end fixity. To determine the total uniform load based on the measured model structural responses, substitute

$$M_{e_m} = M_{1_m} + \frac{P_m b_m}{2} = \frac{E_m I_m \varepsilon_m}{C_m} + \frac{P_m b_m}{2}$$

into Equation (A.10):

$$W_{MODEL} = \frac{12M_{e_m}}{R_m L_m} = \frac{12E_m I_m \varepsilon_m}{C_m (R_m L_m - 6b_m)}$$

which becomes:

$$W_m = 1.1 \times 10^6 \, \varepsilon_m$$

Scaling to prototype values:

$$W_p = 1100 \times 10^6 \, \varepsilon_m$$

this relationship is shown in Figure A.4. Using model strains, estimates of total uniform load are approximately five percent higher than those estimated based on prototype strains.

APPENDIX B

STABILIZER NATURAL FREQUENCY CALCULATIONS

Appendix A showed the SSP stabilizer to act approximately 67 percent fixed, that is, intermediate between fixed and pin-ended. How this might affect the vibrational characteristics of the stabilizer is dealt with in the following calculations which apply to any freely vibrating, partially fixed-ended beam.

Assume the following solution for stabilizer vertical deflection which considers the even (symmetric) modes:

$$Y = \left[A\cos\frac{k\pi x}{L} + B\cosh\frac{k\pi x}{L}\right]\sin\omega t \qquad (B.1)$$

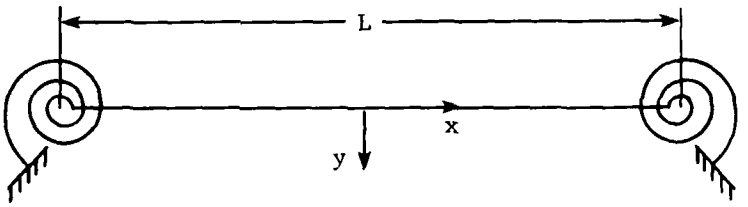

and the following boundary conditions:

$$Y = 0 \text{ at } x = \pm\frac{L}{2} \quad \text{or,} \quad A\cos\frac{k\pi}{2} + B\cosh\frac{k\pi}{2} = 0 \qquad (B.2)$$

at supports:

$$-M = K\left(\frac{dy}{dx}\right) \quad \text{or,} \quad EIy''_{\frac{L}{2}} = -Ky'_{\frac{L}{2}}$$

Then:

$$EI\left(\frac{k\pi}{L}\right)^2\left[-A\cos\frac{k\pi}{2} + B\cosh\frac{k\pi}{2}\right] = -K\frac{k\pi}{2}\left[-A\sin\frac{k\pi}{2} + B\sinh\frac{k\pi}{2}\right]$$

and,

$$A\left[\sin\frac{k\pi}{2} + F\cos\frac{k\pi}{2}\right] + B\left[-F\cosh\frac{k\pi}{2} - \sinh\frac{k\pi}{2}\right] = 0 \qquad (B.3)$$

where,

$$F = \left(\frac{k\pi}{L}\right)\left(\frac{EI}{K}\right) \qquad (B.4)$$

Combining Equations (B.2), (B.3), and (B.4) and simplifying:

$$\tan\frac{k\pi}{2} + \tanh\frac{k\pi}{2} = -\frac{k\pi}{2}\left(\frac{4EI}{KL}\right) \qquad (B.5)$$

Using the relationship developed in Appendix A, this can be expressed in terms of the ratio R through Equation (A.3):

$$R = \frac{KL}{2EI + KL} \quad \text{or,} \quad \frac{KL}{EI} = \frac{2R}{1-R} \qquad (B.6)$$

Thus Equation (B.4) becomes:

$$\tan\frac{k\pi}{2} + \tanh\frac{k\pi}{2} = -\frac{k\pi}{2}\left[\frac{2(1-R)}{R}\right] \qquad (B.7)$$

This is a transcendental function; solution is by an iterative procedure. Now k must be related to W in order to determine the natural frequency. Consider the following beam element:

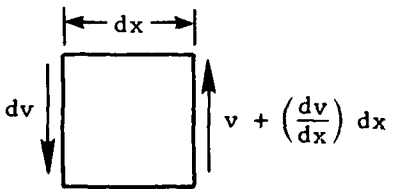

Net vertical force is:

$$\left(\frac{dv}{dx}\right)dx,\ F = ma = m\left(\frac{d^2y}{dx^2}\right)$$

for m use mdx where m is now beam unit density.

$$V = -EI\ddot{y}' \quad \text{and} \quad -EIy^{iv}dx = mdx\ddot{y} \tag{B.8}$$

where $\ddot{y}'$ and $\ddot{y}$ are obtained from Equation (B.1) and then substituted into Equation (B.8) to yield:

$$\omega = \left(\frac{k\pi}{L}\right)^2 \sqrt{\frac{EI}{m}} \tag{B.9}$$

The frequency, f is:

$$f = \frac{\omega}{2\pi} = \frac{k^2\pi}{2L^2}\sqrt{\frac{EI}{m}} \tag{B.10}$$

Now defining a nondimensional factor γ such that:

$$\gamma = \frac{k^2\pi}{2} \tag{B.11}$$

the frequency is as follows:

$$f = \frac{\gamma}{L^2}\sqrt{\frac{EI}{m}} \tag{B.12}$$

The following table summarizes the results of evaluating γ using Equations (B.7) and (B.11) for various values of R. KL/EI is calculated using Equation (B.6). Figure B.1 plots γ as a function of R and KL/EI.

R	KL/EI = 2R/(1-R)	γ
0	0	1.571*
0.1	0.222	1.639
0.2	0.500	1.716
0.3	0.857	1.805
0.4	1.333	1.911
0.5	2.000	2.036
0.6	3.000	2.190
0.7	4.667	2.385
0.8	8.000	2.643
0.9	18.000	3.005
1.0	∞	3.562**

*Note 1.571 = $\pi/2$, pinned beam
**3.5628 fixed beam

From Appendix A, R for the SSP stabilizer was determined to be 0.67. Using this R value and Figure B.1, $\gamma = 2.317$; therefore:

$$f_{SSP} = \frac{2.317}{L^2}\sqrt{\frac{EI}{m}}$$

where $L = 402$ in.
$E = 30 \times 10^6$ psi
$I = 4840$ in.^{4}
m = mass per unit length = weight/gL

In water the so-called "added mass" (the effective mass of water which must be moved in order to permit vibration) predominates the actual mass of the stabilizer itself. For this added mass, use a cylinder of water with diameter equal to the projected width of the stabilizer, which is 93 5/8 inches. This gives the result:

$$m = 0.644 \text{ lb-sec}^2/\text{in.}^2$$

Substituting into Equation (B.13):

$$f_{SSP} = \frac{2.317}{(402)^2}\sqrt{\frac{(30\times10^6)(4840)}{(0.644)}}$$

Then in water:

$$f_{SSP} = 6.8 \text{ Hz}$$

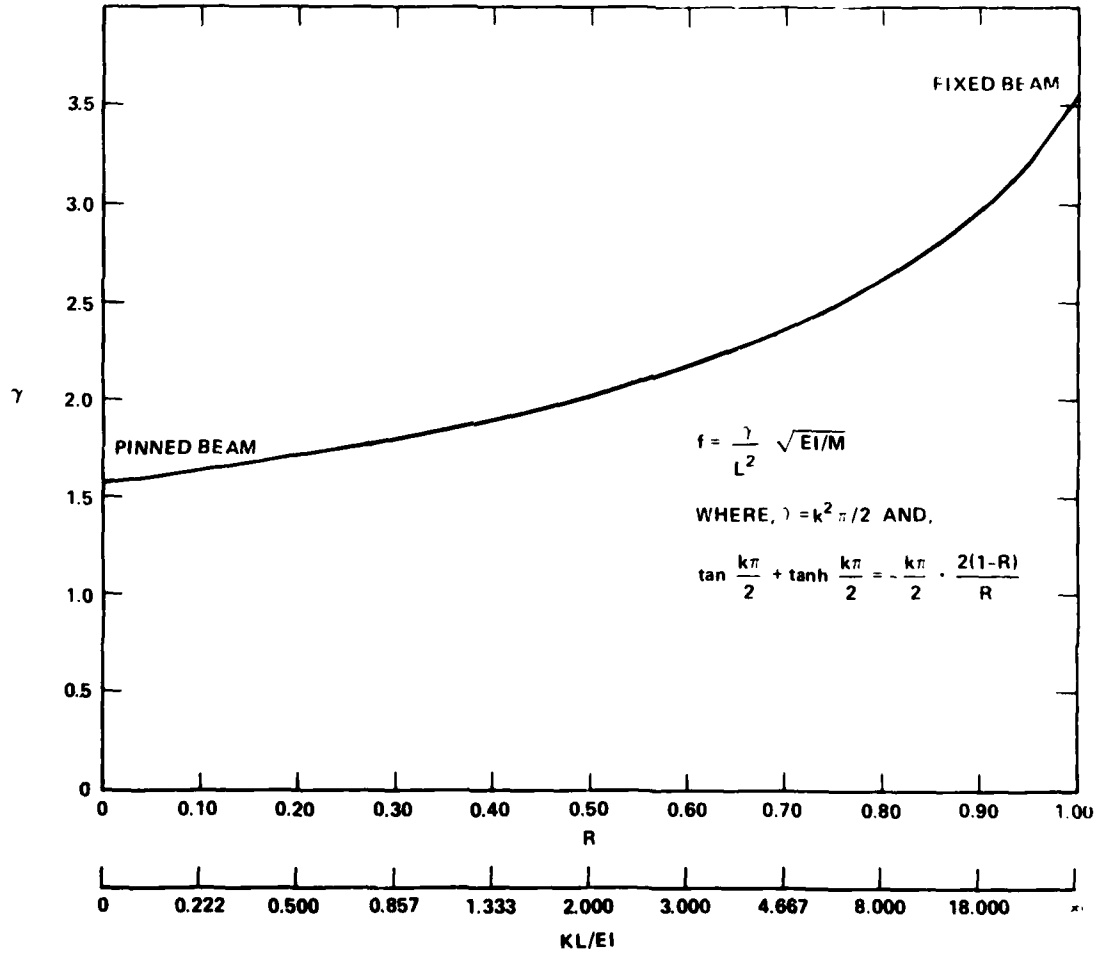

Figure B.1 - Evaluation of "γ"

APPENDIX C

SSP CROSS STRUCTURE BOTTOM STRENGTH IN WAVE IMPACT

A simple strength of materials analysis of the SSP cross structure bottom has been made to determine wave impact pressure at which structural damage may be expected. Table C.1 summarizes calculated uniform pressures that would produce the failure modes for the structural items listed. Point pressures were estimated from the calculated uniform pressures and ratios of peak to average pressures obtained from USNS HAYES (T-AGOR-16) trials and other ship and model experimental data.

The most significant and likely failure modes shown in Table C.1 are C, D, F, G, J, K, and L. Mode C is the onset of permanent deformation of the 4 × 3 × 1/4 stiffeners of the V bow. Mode D is fully plastic bending behavior of the V bow stiffeners, with plastic hinges forming at the truss joints and midspan between joints (Figure C.1). This would be seen as dishing of the stiffeners and plating between joints. Modes F and G are the initiation of yielding and the development of fully plastic hinges in the 6 in. × 4 in. × 3/8 in. transverse stiffener at FR 9, between 8 and 16 feet to starboard of the ship centerline. This would be seen as dishing due to bending of the frame. Modes J and K are the initiation of yielding and the development of fully plastic bending action in the transverse stiffeners in the flat bottom between the deckhouse and open well. This mode will appear as dishing of the bottom grillage in this area. Mode L is plastic shear yielding of these same stiffeners (Figure C.1). Again, this would result in dishing of the entire grillage with high deformation at stiffener supports.

In summary, it is estimated that operating conditions which produce bottom impact point pressures in excess of about 20 psi at the forward V bottom and 10 psi at the flat bottom areas will produce permanent dishing. Single occurrence pressures to produce rupture are beyond the scope of the simple analysis performed, but are known to be substantially higher than the pressures required to cause bending dishing.

PRECEDING PAGE BLANK-NOT FILMED

TABLE C.1 - SSP WAVE IMPACT STRUCTURAL DAMAGE MODES

Mode	Structural Item	Location	Damage Modes	Uniform Pressure (psi)	Point** Pressure (psi)
A	3/8 inch plating	V bow	Initiate bending yield	38	45
B	3/8 inch plating	V bow	Develop three plastic hinges	75	90
C	4 x 3 x 1/4 L	V bow trusses	Initiate bending yield	19	20
*D	4 x 3 x 1/4 L	V bow trusses	Develop three plastic hinges	46	50
E	4 x 3 x 1/4 L	V bow trusses	Initiate bearing yield	42	45
F	6 x 4 x 3/8 L stiffeners	V bow FR 9 stbd	Initiate bending yield	15	20
*G	6 x 4 x 3/8 L stiffeners	V bow FR 9 stbd	Develop three plastic hinges	36	40
H	1/4 inch plate	Flat bottom aft of deckhouse	Initiate bending yield	17	25
I	1/4 inch plate	Flat bottom aft of deckhouse	Develop three plastic hinges	33	50
J	6 x 4 x 3/8 L	Flat bottom aft of deckhouse	Initiate bending yield	4.5	10
*K	6 x 4 x 3/8 L	Flat bottom aft of deckhouse	Develop three plastic hinges	11	20
*L	6 x 4 x 3/8 L	Flat bottom aft of deckhouse	Shear yielding in webs	14	25

*See Figure C1.

**The ratios used to obtain point pressures from calculated uniform pressures were obtained from empirical relationships. These ratios are a function of the size of the pressure bearing area supported by the structural member.

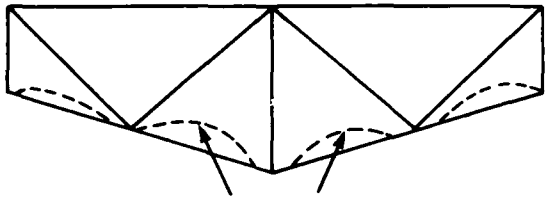

MODE D

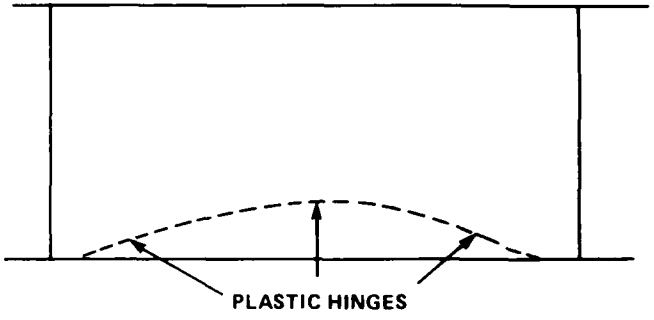

MODE K

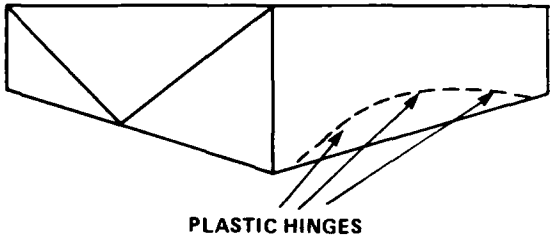

MODE G

VEE BOW DEFORMATION MODES

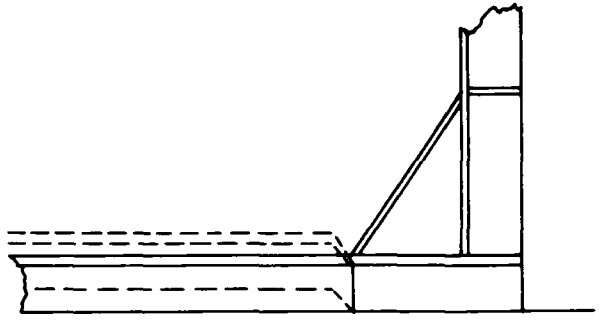

MODE L

FLAT BOTTOM DEFORMATION MODES

Figure C.1 - Structural Deformation Modes

REFERENCES

1. "Navy Completes Semi-Submersible Ship," Ocean Industry, Vol. 8, No. 12 (Dec 1973) pp. 29-35.

2. Stahl, R. and C. Pritchett, "Seaworthiness Characteristics of the Stable Semi-Submerged Platform (SSP)," NSRDC Report 425-H-03 (May 1972).

3. Andrews, J. and A. Dinsenbacher, "Agreement of Model and Prototype Response Amplitude operators and Whipping Response," NSRDC Report 2351 (Apr 1967).

4. Andrews, J. and A. Dinsenbacher, "Structural Response of a Carrier Model in Random and Regular Waves," DTMB Report 2177 (Apr 1966).

5. Kallio, J.A. and M.J. Davis, "Seaworthiness Characteristics of the Stable Semi-Submerged Platform (SSP)," NSRDC Report 425-H-05 (June 1974).

6. Bedore, R.L., "Wave Impact Tests on an SSP Model," NUC TN 1259 (Jan 1974).

7. Fein J.A., "Low Speed Seakeeping Trials of the SSP KAIMALINO," DTNSRDC Report SPD 0650-04 (Mar 1978).

8. Kallio, J.A., "Seakeeping Trials of the Stable Semi-Submerged Platform (SSP KAIMALINO)," DTNSRDC Report SPD 650-03 (Apr 1976).

PRECEDING PAGE BLANK-NOT FILMED

INITIAL DISTRIBUTION

Copies		
4	CNO	
	1	OP 373 (CAPT Hanson)
	1	OP 982F11 (CDR Vaida)
	1	OP 967L
	1	OP 987
1	ASN (RES) (Mantle)	
1	CHNAVMAT/08T23 (Hinton)	
24	NAVSEA	
	3	SEA 03R (Schuler)
	3	SEA 03R (Benen)
	1	SEA 05R
	2	SEA 05R (Vanderveldt)
	5	SEA 312 (Kerr)
	1	SEA 32 (Palermo)
	3	SEA 323 (O'Brien)
	1	SEA 323C (Gagorik)
	5	PMS 383
5	NOSC, HAWAII (HIGHTOWER)	
12	DTIC	

CENTER DISTRIBUTION

Copies	Code	Name
1	11	
15	1110	
1	15	
1	1507	J.A. Fein
1	1536	R.J. Stenson
1	1572	J.A. Kallio
1	17	
1	1706 (m)	
1	173	
1	1730.1	
1	1730.2	
1	1730.3	
20	1730.4	
1	1730.5	
1	1730.5	Dr. M.O. Critchfield
1	1730.6	
1	177 (m)	
10	5211.1	Reports Distribution
1	522.1	Library (C)
1	522.2	Library (A)

PRECEDING PAGE BLANK-NOT FILMED

[redacted]

[redacted] DETERMINATION OF PERMANENT TECH-
[redacted] DISTINCTIVE REGARDLESS OF
[redacted]

[redacted] AND CONCLUSION DETERMINATION OF A PRELIM-
[redacted] OF THE LIMITED INTEREST OR SIGNIFICANCE
[redacted]

[redacted] DISCRIMINATION
[redacted] INTENDED FOR IM-
[redacted] TYPE AND THE
[redacted] OTHERWISE
[redacted] OR A FAMILY CASE


ATE
LME